The effect of the ethanol extract of olive milled waste on allergic reaction of basophil and Ca2+ signal transduction of keratinocyte

岸川, 明日香

The effect of the ethanol extract of olive milled waste on allergic reaction of basophil and Ca^{2+} signal transduction of keratinocyte

Systematic Forest and Forest Products Sciences

Asuka Kishikawa

2017

Table of Contents

Abbreviations

ABTS	3-Ethyl-benzothiazoline-6-sulfonic acid
AD	Atopic dermatitis
Ca^{2+}	Calcium ion
CD_3OD	Deuterated methanol
DCM	Dichloromethane
DMEM	Dulbecco's modified Eagle's medium
DMSO	Dimethyl sulfoxide
DMSO-d_6	Deuterated dimethyl sulfoxide
DNP-BSA	Albumin from Bovine Serum, 2,4-Dinitrophenylated
DPPH	2,2-Diphenyl-1-picrylhydrazyl
EGFP	Enhanced green fluorescent protein
ELISA	Enzyme-linked immunosorbent assay
EMEM	Eagle's minimal essential medium
EtOAc	Ethyl acetate
EtOH	Ethanol
FBS	Fetal bovine serum
GAE	Gallic acid equivalent
Hex	*n*-Hexane
HMBC	Heteronuclear multiple bond correlation
HPLC	High-performance liquid chromatography
HR-ESI-MS	High-resolution electrospray ionization mass spectrometry
HSQC	Heteronuclear single quantum coherence

LC-IT-TOF-MS	Liquid chromatography-ion trap-time of flight-mass spectrometry
MBC	Minimum bactericidal concentration
MeOH	Methanol
MIC	Minimum inhibitory concentration
MPLC	Medium pressure liquid chromatography
MTT	3-(4,5-Dimethylthiazol-2-yl)-2,5-Diphenyltetrazolium Bromide
NMR	Nuclear magnetic resonance
NOESY	Nuclear Overhauser effect spectroscopy
ODS	Octa decyl silyl
OMW	Olive milled waste
ORAC	Oxygen radical absorption capacity
PBS	Phosphate buffered saline
RT-PCR	Real-time polymerase chain reaction
SIRT1	Silent information regulator factor 2 related enzyme 1
SOSA	Superoxide anion scavenging activity
TEAC	Trolox equivalent antioxidant capacity
TLC	Thin-layer chromatography

Introduction

Olive milled waste (OMW) is now expected as a source of natural bioactive compounds in terms of biomass quantity and quality of its content. OMW is by-product of production of virgin olive oil. Though the other plant oils such as soybean oil or rapeseed oil are extracted from plant seeds with additional heat, olive oil is extracted from the fruit itself without additional heat. Usually, olive oil is squeezed from the fruits within a day after harvesting. On extracting olive oil from the fruits, there are several steps: washing, crashing, mlaxation and oil separation from the fruit paste. In order to increase the yield of olive oil and to keep the quality, the fruit processing has been modified several times. For example, a method of two-phase extraction was developed in 1960s, in which the fruit paste is centrifuged and separated into two layers, olive oil and the other part. Traditionally, three-phase extraction was famous, in which the fruit paste was pressed physically and the oil is decanted from liquid phase. The two-phase extraction has been developed because manufacturers can obtain higher olive oil yield. Also, cold press is one of the technique for maintaining taste and nutrient of olive oil. Even they have several choices to increase the yield of olive oil and keep its quality, the production amount of OMW is still much higher than that of olive oil. The production of OMW is more than four times larger than that of olive oil (Ghanbari *et al*., 2012). Moreover, OMW contains 98% of phenolic compound stored in olive fruit, while olive oil contains only 2% of it (Obied *et al*., 2012). The small content of phenolic compound is one of the most important characteristics of olive oil. Olive oil has long been used as not only food but also as folk medicine for skin in Mediterranean countries such as Greece, Spain, Italy, France, Turkey, Palestine, Morocco, Tunisia and Egypt (Ghanbari

et al., 2012). According to several studies including cohort research about relationship between Mediterranean diet and disease of Mediterranean people, consumption of olive oil prevents people from cardiovascular disease (Covas *et al.*, 2006). Also, since ancient period, topical application of olive oil has been common in Mediterranean area for treating dermatitis, eczema, xerosis, other types of inflammation, and photo aging of the skin (Aburjai *et al*., 2003).

Many researchers pointed out these health effects are the benefit of non-saponified minor component dissolving in the oil like phenolic compounds (Ghanbari *et al*., 2012). These non-saponified compounds are partitioned between oil and OMW according to their solubility, and large amount of them remains in OMW during olive oil extraction process (Klen *et al.,* 2012). Though oil extraction methods have been investigated for higher yield and better taste of olive oil, recent progress revealed that depending on the extraction methods, OMW can provide large amount of several useful compounds, such as phenolic compounds, oligosaccharides, triterpenes and more (Fernandez-Hernandez *et al.*, 2015). Unlike the other plant oil, olive oil is easily extracted by squeezing or centrifugation and additional heat is not needed.

fruit paste malaxation (i.e., churning or mixing) performed to obtain higher olive oil yields sets off various enzymatic and/or chemical reactions such as oxidation, glycosidation and hydrolysis of the glycosidic bonds, and as a result, versatile modified compounds are naturally produced (Cardoso et al. 2011; Klen et al. 2012). OMW is thus now regarded as a potential source of useful natural compounds.

Oleuropein and hydroxytyrosol are the well-known active phenolic compounds of the olive. According to the previous reports related to skin remedy, oleuropein

inhibited the skin thickness and DNA damage induced by UV when it was administered orally to mice (Sumiyoshi *et al*., 2010). Also, oleuropein inhibited inflammatory cell recruitment and the release of inflammatory cytokines (Giner *et al*., 2013). Hydroxytyrosol upregulated heme oxygenase-1, which is an antioxidant enzyme, in keratinocyte, indicating that it could have a radio-protective effect on human skin (Rafehi *et al*., 2012). Oleuropein and hydroxytyrosol have been found not only from olive oil, but also from OMW, leaves and wooden parts (Klen *et al*. 2012; Perez-Bonilla *et al*. 2006).

Scientific evidence about the functional aspects of natural product leads us to utilize the natural source as a sustainable resource. However, the knowledge about functionality of extract of OMW and its active compounds is limited. Therefore, the purpose of this research is to investigate biological activities of the extract of OMW on skin related cells and to identify its active compounds for more utilization of OMW.

Chapter 1: Chemical properties of the extracts of OMW and each part of the olive

1-1. Introduction

The extractives from plant contain primary metabolite and secondary metabolite, such as fatty acids, sugars, polyphenols, terpenoids and so on. Some metabolites have specific functional effects on human body and are used for treatment or prevention of diseases. As for olive, oleuropein and hydroxytyrosol are the famous secondary metabolites, because they contribute taste and biological activities of olive oil. In order to evaluate biological activities of extractives of OMW, two kinds of extract with different chemical characteristic, ethanol (EtOH) extract and water extract, were prepared. Also, the extracts of each parts of olive were prepared in the same way as OMW to compare their biological activities. The composition of OMW varies depending on olive cultivar and olive oil extraction. To know general information of the extracts, each content of oleuropein and hydroxytyrosol was analyzed by HPLC and LC/MS analysis, the total phenol (TP) content was measured by Folin-Ciocalteu assay, and antioxidant activities were estimated by four kinds of methods.

1-2. Materials

Fresh OMW, fruit pulp, seeds, leaves, stems and flowers were collected on Kyushu Island in 2013. OMW and olive fruits were collected in October (mixture of Mission, Manzanillo, Nevadillo Blanco and Lucca cultivars). Fruits were squeezed freshly using a two-phase centrifuge, and OMW was collected soon after the separation

from the oil. Fruits were divided into two parts to make fruit pulp and seeds. Leaves and stems (Mission cultivar) were collected at two different seasonal stages, May (flowering time) and October (fruit harvesting time). Flowers (Mission cultivar) were collected in May.

1-3. Extraction with EtOH or water

Methods: Soon after sample collection, each part was freeze-dried and milled into powder, and extracted with 99.5% ethanol (EtOH) or water on a shaker at 200 rpm at room temperature for 24 h. Then the extraction yield was calculated after EtOH extracts were concentrated and dried using a rotary evaporator, and the water extracts were freeze-dried.

Results: Table 1 shows the ratio of extraction solvent (EtOH and water) versus dried raw material and the extraction yield. The extraction yields from OMW, fruit pulp, and seeds were relatively higher than those from leaves, stems and flowers because the former parts contained oil.

Table 1 The amount of extraction solvent and the extraction yield of (a) EtOH extracts and (b) water extracts of OMW and each part of the olive

(a)

EtOH extract	Extraction	
	Solvent (mL/g of dry weight)	Yield (g/g of dry weight×100)
OMW	10.0	18.3
Fruit pulp	10.0	37.2
Seeds	10.0	9.2
Leaves (May)	6.7	4.8
Leaves (Oct.)	10.0	12.7
Stems (May)	4.8	3.2
Stems (Oct.)	10.0	5.5
Flowers	14.0	6.9

(b)

Water extract	Extraction	
	Solvent (mL/g of dry weight)	Yield (g/g of dry weight×100)
OMW	10.0	18.4
Fruit pulp	10.0	25.3
Seeds	10.0	4.0
Leaves (May)	6.7	12.7
Leaves (Oct.)	10.0	7.5
Stems (May)	3.3	6.9
Stems (Oct.)	10.0	10.6
Flowers	11.1	17.9

1-4. **HPLC and LC/MS analysis**

Methods: For HPLC and LC/MS analysis, the EtOH extracts, oleuropein, and hydroxytyrosol were dissolved in EtOH, and the water extracts were dissolved in water. The concentration of the extracts was set at 1 μg/mL. HPLC analysis was performed on a CAPCELL PAK C_{18} UG120 (5 μm, 4.6 mm I.D. × 250 mm, Shiseido, JAPAN) under the following conditions: column temperature, 40 ºC; flow rate, 1.0 mL/min; injection volume, 10 μL; elution solvents, (A) acetonitrile and (B) formic acid (0.1%) in water; mobile phase program, a linear gradient elution of 5%-30% (A) for the first 30 min followed by an isocratic elution of 30% (A) for 10 min; detection wave lengths, 280 nm and 380 nm. LC/MS (ESI) analysis was conducted using a CAPCELL PAK C18 UG120 (3 μm, 2.0 mm I.D. × 150 mm, Shiseido, JAPAN). The flow rate was 0.2 mL/min, the injection volume was 5 μL, the ion polarity was in negative mode, and the other analytical conditions were the same as in the HPLC analysis. The chromatogram of each extract was compared with that of oleuropein or hydroxytyrosol.

Results: Fig. 1 shows the HPLC chromatograph of the EtOH extracts at 280 nm. Standards of oleuropein and hydroxytyrosol were detected by HPLC at 280 nm with retention times of 30.4 min and 8.7 min, respectively. A peak at 30.4 min appeared in EtOH extract from the leaves (May and Oct.), stems (May and Oct.), and flowers, but there was no extract which contains a peak at 8.7 min. The peaks at 30.4 min was confirmed to be oleuropein by further LC/MS analysis, as a deprotonated molecular ion peak at m/z 538.8 $[M-H]^-$. Table 2 shows the estimated content of oleuropein in the EtOH extracts. The amounts of oleuropein in the EtOH extract of leaves (May and Oct.), stems (May and Oct.), and flowers were then determined to be 56.2, 174, 189, 246 and

33.4 mg/g in the extracts, respectively. On the other hand, oleuropein was not detected in the EtOH extracts of OMW, fruit pulp, or seeds nor in any of the water extracts. Oleuropein in fruit is converted gradually to dimethyloleuropein or elenolic acid glucoside after the fruit enters the mature stage (Romero *et al*., 2002). October is the last maturation stage for olive fruits in Japan, so oleuropein may be not detected in the fruit samples. The oleuropein content of the EtOH extract of the stems (Oct.) was the highest (246 mg/g) among all the extracts. However, the oleuropein content of raw dried material was highest (22.1 mg/g) in the leaves (Oct.) as it might have the highest extraction yield. Because oleuropein is one of the most famous bioactive compounds in olive oil, biological activities of oleuropein were also evaluated in the following bioassays to know whether it contributes the activity of the extracts or not.

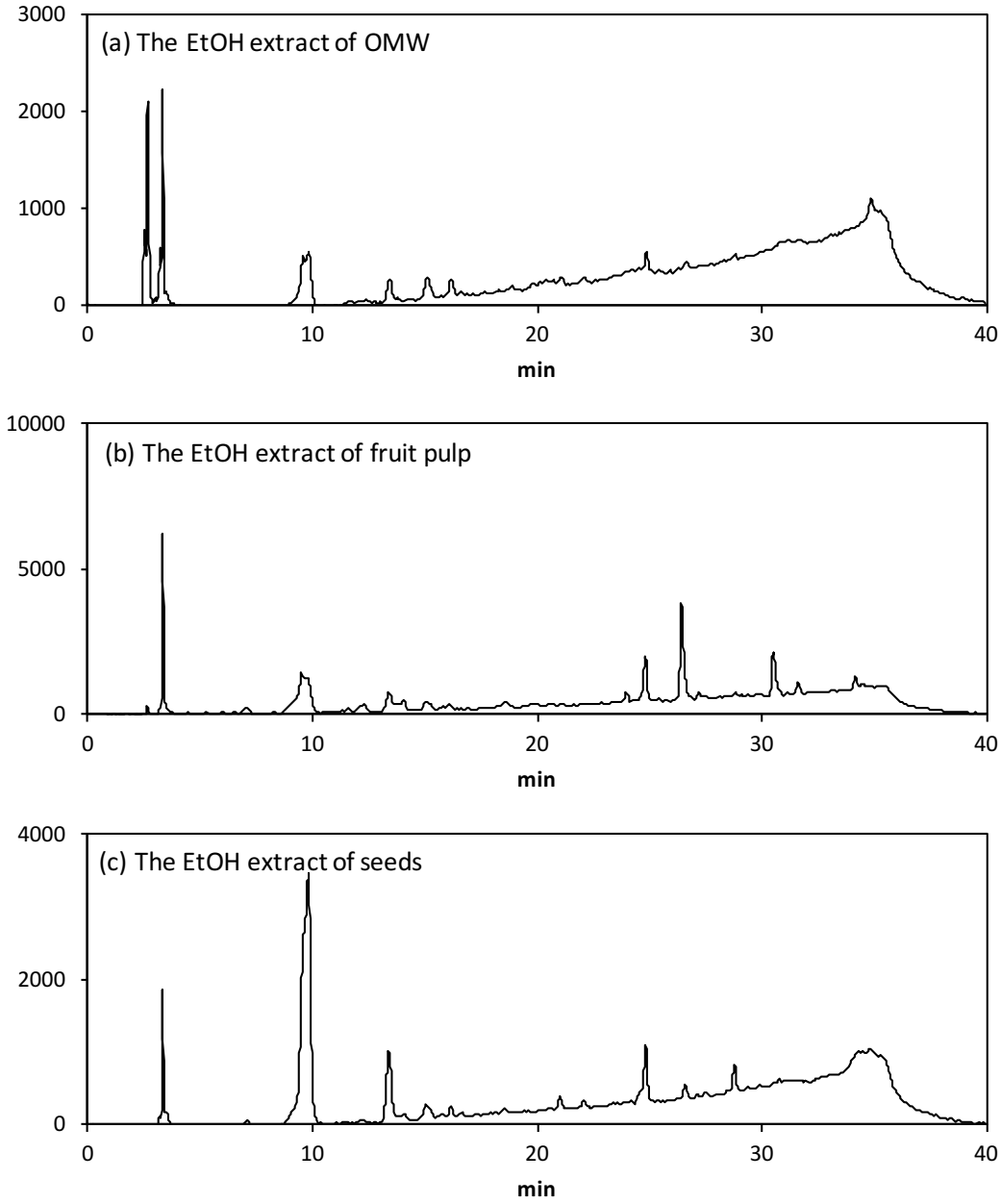

Fig. 1 (a)-(c) HPLC chromatograms at 280 nm of the EtOH extract of (a) OMW, (b) fruit pulp, (c) seeds, (d) leaves (May), (e) leaves (Oct.), (f) stems (May), (g) stems (Oct.) and (h) flowers.

The peak of oleuropein was detected at 30.4 min in the current linear gradient system: (A) acetonitrile : (B) formic acid (0.1%) in water = 5 : 95 (0 min) to 30 : 70 (30-40 min) with an HPLC column, CAPCELL PAK C18 UG120.

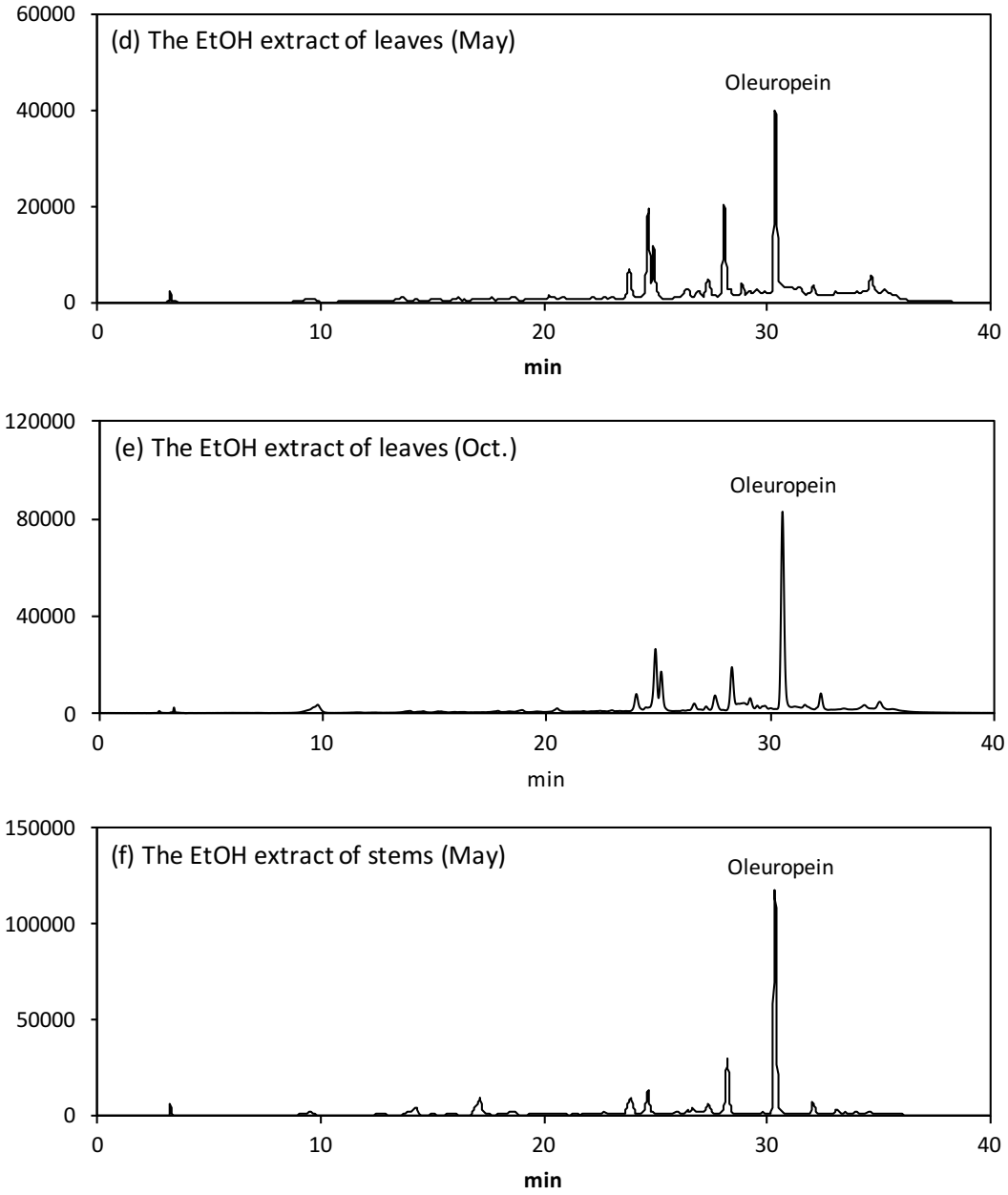

Fig. 1 (d)-(f) HPLC chromatograms at 280 nm of the EtOH extract of (a) OMW, (b) fruit pulp, (c) seeds, (d) leaves (May), (e) leaves (Oct.), (f) stems (May), (g) stems (Oct.) and (h) flowers.

The peak of oleuropein was detected at 30.4 min in the current linear gradient system: (A) acetonitrile : (B) formic acid (0.1%) in water = 5 : 95 (0 min) to 30 : 70 (30-40 min) with an HPLC column, CAPCELL PAK C18 UG120.

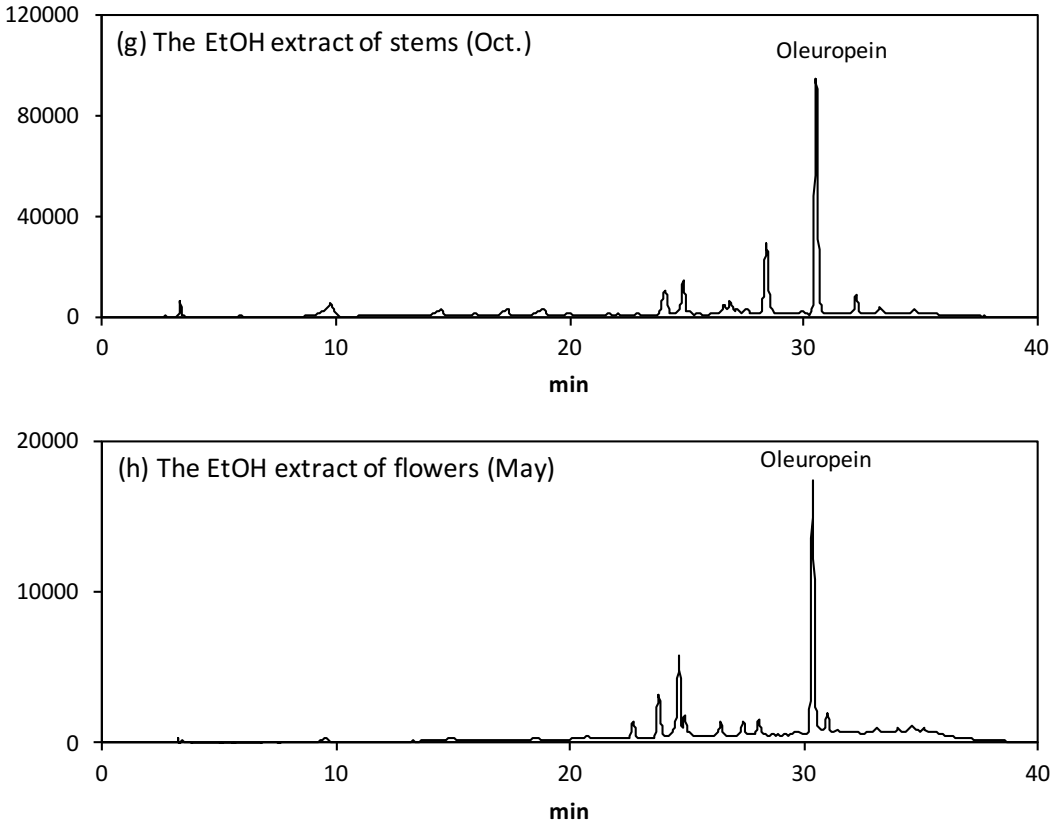

Fig. 1 (g)-(h) HPLC chromatograms at 280 nm of the EtOH extract of (a) OMW, (b) fruit pulp, (c) seeds, (d) leaves (May), (e) leaves (Oct.), (f) stems (May), (g) stems (Oct.) and (h) flowers.

The peak of oleuropein was detected at 30.4 min in the current linear gradient system: (A) acetonitrile : (B) formic acid (0.1%) in water = 5 : 95 (0 min) to 30 : 70 (30-40 min) with an HPLC column, CAPCELL PAK C18 UG120.

Table 2 Oleuropein content (mg/g) of the EtOH extracts and water extracts per extract amount or per dry weight of the materials.

EtOH extract	EtOH extract		Water extract	
	mg/g of extract	mg/g of dry weight	mg/g of extract	mg/g of dry weight
OMW	-	-	-	-
Fruit pulp	-	-	-	-
Seeds	-	-	-	-
Leaves (May)	56.2	2.7	-	-
Leaves (Oct.)	174	22.1	-	-
Stems (May)	189	6.0	-	-
Stems (Oct.)	246	13.5	-	-
Flowers	33.4	2.3	-	-

-: Not detected.

1-5. Total phenol content

Total phenol (TP) content was determined using the Folin-Ciocalteu assay. Fifty microliter of sample solution (2 mg/mL or 4 mg/mL) was mixed with 100 μL of Folin-Ciocalteu reagent. After 3 min mixing, 400 μL of 7.5% sodium carbonate solution was added to the mixture. After a 2-h reaction, the absorbance was measured at 765 nm. Finally, the TP content was calculated as a gallic acid equivalent (mg GAE/g) (n=3).

Table 3 shows the TP content in each extract or in the dry weight of the material. All the extracts were estimated to contain phenolic compounds. Of the EtOH extracts, the stems (May and Oct.) showed the highest TP content (169.7 and 165.3 mg GAE/g, respectively, in the extract) followed by the leaves (May and Oct.), flowers, seeds, fruit pulp, and OMW. Of the water extracts, the seeds showed the highest TP content (46.8 mg GAE/g in the extract) followed by the fruit pulp, stems (Oct.), OMW, stems (May), leaves (May and Oct.) and flowers. The EtOH extracts of stems (May and Oct.), leaves (May and Oct.) and flowers were the only extracts to contain a high TP content over 50 mg GAE/g. TP content of the water extract was relatively lower than that of the corresponding EtOH extract. It is because of the polarity of the extraction solvent, that is, EtOH can extract more hydrophobic compounds like polyphenol, and water can extract more hydrophilic compounds like sugar.

Table 3 The total phenol (TP) content of (a) EtOH extracts and (b) water extracts of OMW and each part of the olive.

(a)

EtOH extract	TP content (mg GAE/g)	
	in extract	in dry weight
OMW	22.8	4.2
Fruit pulp	23.9	8.9
Seeds	27.5	2.5
Leaves (May)	100.7	4.8
Leaves (Oct.)	117.6	14.9
Stems (May)	169.7	5.4
Stems (Oct.)	165.3	9.1
Flowers	81.6	5.6

(b)

Water extract	TP content (mg GAE/g)	
	in extract	in dry weight
OMW	34.9	6.4
Fruit pulp	43.8	11.1
Seeds	46.8	1.9
Leaves (May)	22.6	2.9
Leaves (Oct.)	21.0	1.6
Stems (May)	23.5	1.6
Stems (Oct.)	39.2	4.2
Flowers	21.0	3.8

1-6. **Antioxidant assay**

The antioxidant activities of the samples were estimated by ABTS (3-ethyl-benzothiazoline-6-sulfonic acid) assay, DPPH (2,2-diphenyl-1-picrylhydrazyl) assay, oxygen radical absorption capacity (ORAC) assay, and superoxide anion scavenging activity (SOSA) assay.

The ABTS assay described previously (Tanaka *et al*., 2014) was performed to measure the ABTS radical scavenging activity of the samples. In order to make a standard curve, 1 mL of the working solution was mixed with 100 mL of Trolox solution, and the mixture was incubated at 30°C for 4 min. Instead of Trolox, each sample was added to the working solution by the same method. The results are expressed in terms of Trolox equivalent antioxidant capacity (TEAC) (μg/mg).

The DPPH assay described previously (Thaipong *et al*., 2006) was performed to measure the DPPH radical scavenging activity of the samples. Trolox was used for a standard curve. One milliliter of Trolox solution in Tris-HCl Buffer (0.1 M) was allowed to react with 1 mL of DPPH solution (0.2 mM) for 30 min. Instead of Trolox, each sample was added to the DPPH solution. The results were expressed in terms of TEAC (μg/mg).

The ORAC assay described previously (Mira *et al*., 2013) was performed to measure the peroxyl radical scavenging activity of the samples. Data were expressed as micromoles of TEAC (μmol TE/mg).

These three TEAC values were determined using the following mathematical expression: TEAC = [IC_{50} of Trolox] / [IC_{50} of sample].

SOSA was performed as described previously (Tanaka *et al*., 2014). Kit-WST

(Dojindo, JAPAN, S311) was used in this assay. Data were expressed in terms of SOD equivalent antioxidant capacity (U/μg extract).

Table 4 shows the antioxidant activities of the EtOH extracts, oleuropein, and the water extracts. The antioxidant activity of the sample was considered 'not detectable' when its IC_{50} was higher than the maximum solubility. In EtOH extracts, leaves, stems, and flowers showed relatively higher antioxidant activities than OMW, fruit pulp, and seeds. This could be one of the reasons for the high antioxidant activities of the leaves, stems, and flowers. Generally, the catechol moiety in the polyphenol structure has strong reducing power and shows antioxidant activity. Oleuropein, one of the polyphenols in olives, showed antioxidant activity (ABTS, 424.5 μg/mg; DPPH, 612.9 μg/mg; ORAC, 3.69 μmol TE/mg; SOSA, 2.00 U/μg). The highest content of oleuropein in stems (Oct.) might participate in the highest antioxidant activity of the EtOH extract in the ABTS (271.0 μg/mg) and SOSA assays (1.12 U/μg).

Some antioxidant activity, however, had no correlation with the oleuropein content or TP content. For example, the antioxidant activity of the leaves (May) was lower than that of the leaves (Oct.) in the ABTS and DPPH assays. On the other hand, the antioxidant activity of the leaves (May) was higher than that of the leaves (Oct.) in the ORAC and SOSA assays, even though the TP content of the leaves (May) was lower than that of the leaves (Oct.). These uncorrelated results were caused by seasonal variation of the components in the extracts and differences in principal among the four antioxidant assays. In a previous report, which compared the antioxidant activity of immature and mature olive leaves, DPPH radical scavenging activity correlated with the TP content of the olive leaf extract; however, ABTS radical scavenging activity did not

correlate with the TP content in this way (Brahmi *et al*., 2013).

The water extracts of seeds, stems (Oct.), and fruit pulp showed higher ABTS radical scavenging activity than the other water extracts. According to the Folin-Ciocalteu assay, the TP content of the water extracts of seeds, stems (Oct.), and fruit pulp was higher than that of the other water extracts. It is likely that the three water extracts showed high ABTS radical scavenging activity because of their high TP content.

Oxidative stress in the skin induced by UV irradiation results in conditions associated with photo aging, such as damaged DNA and skin cancer (Budiyanto *et al*., 2000) and inflammation activation of melanin synthesis (Ha *et al*., 2009). Antioxidant activity is one of the effective characteristic of skin treatment agent.

Table 4 Antioxidant activity (ABTS, DPPH, ORAC and WST-1) of (a) EtOH extracts and (b) water extracts of OMW and each part of the olive.

(a)

EtOH extract	ABTS TEAC (μg/mg)	DPPH TEAC (μg/mg)	ORAC TEAC (μmol TE/mg)	WST-1 SOSA (U/μg)
OMW	-	-	0.08 ± 0.00	0.20 ± 0.0
Fruit pulp	-	-	0.03 ± 0.00	0.14 ± 0.0
Seeds	-	-	0.11 ± 0.00	0.48 ± 0.1
Leaves (May)	55.0 ± 1.9	189.2 ± 0.9	2.12 ± 0.08	0.70 ± 35
Leaves (Oct.)	168.9 ± 2.2	289.6±25	0.47 ± 0.01	0.25 ± 0.1
Stems (May)	101.1 ± 1.9	302.2 ± 21	2.94 ± 0.08	0.45 ± 16
Stems (Oct.)	271.0 ± 4.4	239.1±6.6	1.25 ± 0.00	1.12 ± 0.3
Flowers	51.8 ± 1.2	185.2 ± 2.8	1.72 ± 0.08	0.69 ± 85
Oleuropein	424.5±3.1	612.9±31	3.69±0.01	2.00±0.2

The antioxidant values are presented as means±SD (n=3).

− : not detectable.

TEAC : Trolox equivalent antioxidant capacity.

SOSA : superoxide anion-scavenging activity.

Table 4 (b)

Water extract	ABTS TEAC (μg/mg)	DPPH TEAC (μg/mg)	ORAC TEAC (μmol TE/mg)	WST-1 SOSA (U/μg)
Leaves (May)	-	-	0.42 ± 0.02	0.04 ± 12
Leaves (Oct.)	-	-	0.12 ± 0.01	0.05 ± 0.0
Stems (May)	-	-	0.75 ± 0.01	0.08 ± 5.8
Stems (Oct.)	88.5 ± 1.9	-	0.08 ± 0.00	0.04± 0.0
Flowers	-	-	0.54 ± 0.04	-
OMW	-	-	0.19 ± 0.01	0.34 ± 0.1
Fruit pulp	75.5 ± 2.0	-	0.57 ± 0.01	0.17 ± 0.0
Seeds	133.4 ± 18	-	0.17 ± 0.00	0.16 ± 0.1

The antioxidant values are presented as means±SD (n=3).

− : not detectable.

TEAC : Trolox equivalent antioxidant capacity.

SOSA : superoxide anion-scavenging activity.

Chapter 2: Evaluation of the biological activities of the crude extracts on skin related factors

2-1. Introduction

In this chapter, the potential of the extractives of OMW and each part of the olive for use as skin treatments or antiaging is discussed basing on some *in vitro* bioactive assays. Popular uses for skin treatments include preventing bacterial infection like folliculitis or impetigo, skin lightening, removing skin wrinkles, inhibiting allergic reaction, keeping intact barrier structure of epidermis and so on. In order to estimate the ability of the extracts to fulfill the functions, several *in vitro* assays were conducted such as antibacterial assay, anti-melanogenesis assay, collagen-production-promoting assay, anti-allergic assay, and keratinocyte stimulating assay. These screening results suggested potential of the extractives for use in skin treatment and necessity of further research for application.

2-2. Materials

Staphylococcus aureus (NBRC, 12732) and *Escherichia coli* (NBRC, 3301) were purchased from the NITE Biological Resource Center (NBRC, Chiba, JAPAN).

B16 melanoma cells and rat basophilic leukemia (RBL-2H3) cells (Riken Bioresource Center, Japan) were routinely maintained in 10% FBS in Eagle's minimal essential medium (EMEM). HaCaT, a cell line of human keratinocyte, and Adult normal human dermal fibroblasts (NHDF-Ad, Lonza, Tokyo, Japan) were routinely maintained in 10% FBS in Dulbecco's modified Eagle's medium (DMEM). All of the cultivation

was conducted at 37°C, 5.0% CO_2.

MTT (3-(4,5-dimethylthiazol-2-yl)-2,5-diphenyltetrazolium bromide) reagent was purchased from Tokyo Chemical Industry (Tokyo, Japan). A human collagen type I ELISA kit was purchased from ACEL (Kanagawa, Japan). Hoechst 33342 and a Ca^{2+} probe kit, Fluo-4 AM, were purchased from Dojindo (Kumamoto, Japan). High Pure RNA isolation Kit was purchased from Roche (Basel, Switzerland). ReverTra Ace kit was purchased from Toyobo (Osaka, Japan).

2-3. Sample preparation

To prepare the samples for the following biological assays, EtOH extracts and oleuropein were dissolved in DMSO, and water extracts were dissolved in distilled water.

2-4. Statistical analysis

The results are expressed as means ± standard deviation (n=3). Significant differences between each tested group and the control group were determined using Dunnett's multiple post hoc test (* $p<0.05$, ** $p<0.01$), when the one-way analysis of variance (ANOVA) was significant ($^a p<0.01$).

2-5. Antibacterial activity

S. aureus and *E. coli* inhabit on our skin and soft tissue, and they are one of the cause of skin infection or allergic disease. *S. aureus* is a major cause of skin infection such as impetigo and folliculitis in both developed and developing countries.

Recent reports showed that involvement of *S. aureus* infection to atopic dermatitis (AD) because larger amount of S. aureus was found on AD skin (Miller *et al*., 2011). Antibacterial activity against *S. aureus* and *E. coli* was determined.

The assay described previously (Tanaka *et al*., 2014) was performed with slight modification. A single colony of *S. aureus* or *E. coli* was taken from nutrient agar plate and it was maintained in 5 mL of NB medium. The bacteria were cultured at 37 °C ± 1 °C with shaking at 120 rpm for one day. The culture medium was then diluted with fresh NB medium to make the exact concentration at 10^4 CFU/mL by measuring its turbidity (OD_{630}). The bacterial suspension was used in the antibacterial assay. The tested EtOH extracts were dissolved in DMSO, and the tested water extracts were dissolved in sterilized distilled water at the maximum solubility. Into each well of a 96-well plate were added 150 µL of test solution containing 133.5 µL of fresh NB medium, 15 µL of bacteria suspension, and 1.5 µL of DMSO or sterilized distilled water with or without each sample. Also, instead of 15 µL of bacteria suspension, 15 µL of fresh NB medium was added into test solution of a blank well. The blank well, which was used for subtraction of the absorption at 630 nm of the tested sample, was prepared as it corresponds to each sample. Sorbic acid (400 µg/mL) was used as a positive control, and the sample solvent was used as a negative control. After 18-h incubation at 37 °C ± 1 °C with shaking at 1160 rpm, bacterial growth was determined with OD_{630} measured by a microplate reader (Biotek-ELX800, BioTek) as follows:

$$\text{Bacterial growth (\%)} = \frac{OD630_{\,test} - OD630_{test\,BL}}{OD630_{\,control} - OD630_{control\,BL}} \times 100$$

where $OD630_{test}$ is OD_{630} of the test well (bacteria: +, sample:+), $OD630_{test\,BL}$ is OD_{630}

of a blank well corresponding to the test well (bacteria: -, sample:+), $OD630_{control}$ is OD_{630} of a control well (bacteria: +, sample: -), $OD630_{control\ BL}$ is OD_{630} of a blank well for a control (bacteria: -, sample:-).

When the sample have the inhibitory effect of bacterial growth, the minimum inhibitory concentration (MIC), which is the lowest concentration of the sample required to completely inhibit the growth of a particular bacteria, and the minimum bactericidal concentration (MBC), which is the lowest concentration of the sample required to kill the bacteria, were measured. The MIC of antibacterial samples were determined by measuring the bacterial growth written above with several concentrations of the active sample. The MBC of the active samples were evaluated as follows: 20 μL of the test solution was taken from the active well of the 96-well plate and diluted for ten times with 180 μL of fresh NB medium. An aliquot of 100 μL of the diluted solution was spread on the surface of a nutrient agar plate and sealed with plastic paraffin film. After 18 h incubation at 37 °C ± 1 °C, the formation of colonies of the bacteria was observed. And the lowest concentration of the sample that leaded no colony formation on the nutrient agar plate was determined as the MBC.

Table 5 shows the effects of EtOH extracts, oleuropein, and water extracts on antibacterial activity against *S. aureus* and *E. coli.* None of the extracts inhibited the growth of *E. coli*; however, EtOH extracts of leaves (May and Oct.) and flowers inhibited the growth of *S. aureus.* The MICs of the active samples were 800 μg/mL, and the MBC of the EtOH extract of flowers was 1600 μg/mL. Oleuropein, which was contained in the EtOH extracts of leaves and flowers, showed no inhibition effect on the bacterial growth, so the active compound for the antibacterial activity of the extracts

might not be oleuropein.

The EtOH extract of the leaves and flowers were found to be anti *S. aureus* agents. *S. aureus* is one of the major cause of skin infection disease and AD. Further research is needed to investigate treating methods using those active extracts.

Table 5 The effect of (a) EtOH extracts and (b) water extracts of OMW and each part of the olive on growth of *E. coli* and *S. aureus*.

(a)

		S. aureus			*E. coli*
EtOH extract	**(μg/mL)**	**OD630 (%)**	**MIC (μg/mL)**	**MBC (μg/mL)**	**OD630 (%)**
Control		100±3.6			100±1.3
Sorbic acid	**400**	0.00±0.0			0.35±0.1
OMW	**900**	116±6.7	-	-	94.3±3.3
Fruit pulp	**900**	97.1±19	-	-	111±1.9
Seeds	**900**	99.0±7.0	-	-	66.0±8.2
Leaves (May)	**800**	0.00±0.0	800	-	64.7±8.3
Leaves (Oct.)	**800**	0.00±2.7	800	-	86.5±3.4
Stems (May)	**1600**	112±1.9	-	-	82.7±6.8
Stems (Oct.)	**800**	88.4±4.6	-	-	88.8±18
Flowers	**800**	0.00±0.0	800	1600	74.1±2.9
Oleuropein	**700**	98.9±0.3	-	-	81.0±3.2

Sorbic acid: positive control.

MIC: minimum inhibitory concentration, MBC: minimum bactericidal concentration.

The relative activity values (mean±SD) were normalized to the control (n=3).

(b)

Water extract	(µg/mL)	*S. aureus*	*E. coli*
		OD630 (%)	**OD630 (%)**
Control		100±4.4	100±1.2
Sorbic acid	**400**	0.00±0.0	0.35±0.1
OMW	**400**	140±46	98.8±4.5
Fruit pulp	**400**	106±21	96.0±5.6
Seeds	**400**	166±17	91.1±2.9
Leaves (May)	**1600**	116±4.6	92.5±18
Leaves (Oct.)	**400**	118±21	123±1.1
Stems (May)	**800**	152±1.6	129±2.1
Stems (Oct.)	**800**	130±21	128±0.8
Flowers	**800**	180±5.5	114±19

Sorbic acid: positive control.

MIC: minimum inhibitory concentration, MBC: minimum bactericidal concentration.

The relative activity values (mean±SD) were normalized to the control (n=3).

2-6. Determination of non-cytotoxic concentrations for cell lines

In order to determine the concentration of the extracts used in further cell experiments, the cell viability (CV) of cells (B16 melanoma, NHDF-Ad, RBL-2H3 and HaCaT cell) treated with the samples was measured using MTT assay (Tanaka *et al*., 2014). The cells were treated with the extracts at the maximum solubility of the sample and its several diluted concentrations. The methods by which the cells were treated with samples are described in each assay's section. After the sample treatment, the medium containing the sample was removed and the cells were rinsed with PBS. An aliquot of each medium containing 0.5 mg/mL of MTT reagent was added. After 4 h incubation, the formazan crystal formed in the living cells were dissolved in 0.1 M HCl in isopropanol, and then the absorbance at 570 nm of the solution was measured. The CV was calculated as follows:

$$\text{CV}\ (\%) = \frac{Abs570_{test}}{Abs570_{cont.}} \times 100$$

where $Abs570_{test}$ was the absorbance at 570 nm of the tested well (sample: +) and $Abs570_{cont.}$ was the absorbance at 570 nm of a control well (solvent for the sample: +). Then the maximum soluble concentration of the sample at which CV was higher than 90% was defined as the non-cytotoxic concentration. Extracts were added to the cells at the non-cytotoxic concentration in further cell experiments.

The concentrations of the samples are given in Table 6, 7, 8 and 9, and a superscript '+' was attached to any non-cytotoxic concentrations that were equal to the maximum solubility.

2-7. Anti-melanogenesis activity

Melanin produced by melanocytes is the cause of aging spots and darkness of the skin. The assay described previously (Arung *et al*., 2007) was performed to screen for inhibitors of melanin synthesis in melanocytes. B16 cells, which are a tumor analog of mice melanocytes, were used as a model cell of melanocyte.

B16 cells were seeded on 24-well plates (1×10^5 cells/well) with 1 mL of EMEM containing 90 μg/mL theophylline and 10% FBS. The medium was replaced with a mixture of 998 μL of fresh EMEM and 2 μL of the sample in 24-h and 72-h incubation periods. The absorbance of melanin in 1 M NaOH cell lysate was measured at 405 nm in a 96-h incubation period for calculating the melanin content (MC). CV was measured using MTT assay. The solvent (water or DMSO) used for dissolving the sample was used as a corresponding control, and arbutin (final concentration: 100 μg/mL) was used as a positive control.

Table 6 shows the effects of EtOH extracts, oleuropein, and water extracts on MC in B16 cells and CV. The MC and CV levels of the controls were set at 100%. A low MC value means that the sample has anti-melanogenesis activity. As shown in Table 4 (a), oleuropein and all the EtOH extracts except for those from seeds showed significant differences from the control group. In particular, the EtOH extracts of leaves (May) strongly inhibited melanogenesis (the MC was 31.8%). Oleuropein also showed this same activity (the MC was 58.4%). None of the water extracts showed a significant difference from the control in terms of their anti-melanogenesis effects. As for the effect of oleuropein, it is possible for oleuropein to partially contribute to the activity of some EtOH extracts. However, there was little correlation between the activity strength and

oleuropein content of these extracts. For example, comparing the MC value of each EtOH extract at the same concentration, 20 μg/mL, which showed no cytotoxicity, leaves (May), leaves (Oct.), stems (Oct.), and flowers gave the MC value of 58.4 ± 6.7%, 80.7 ± 2.9%, 86.2 ± 5.8%, and 83.4 ± 2.0% respectively. The other EtOH extracts gave the MC value over 90% at 20 μg/mL. From these results, we can see that in spite of lower amount of oleuropein content shown in Table 1 (a), EtOH extract of leaves (May) has the strongest anti-melanogenesis activity. There are several possibilities regarding the mechanism of anti-melanogenesis activity. One possible reason for this was that the compounds had a synergistic effect. The synergistic effect of oleuropein and flavonoids was described previously, and olive leaf extract showed anti-cancer activity in B16 cells at concentrations higher than 150 μg/mL (Mijatovic *et al*., 2010). In our experiment, synergistic effects were also expected to result in strong anti-melanogenesis activity of EtOH extract of leaves (May) at non-cytotoxic concentrations. Another reason for this was that there existed some other effective compounds than oleuropein.

Excessed melanin production causes skin darkness and aging spots. However, melanin is necessary to protect skin from harmful UV light. To remove these pigmentations and keep skin health, it is important to reduce melanin production in melanocyte without cytotoxicity.

Table 6 The effect of (a) EtOH extracts and (b) water extracts of OMW and each part of the olive on melanin synthesis in B16 cells and cell viability.

(a)

	B16 melanoma		
	EtOH extract		
	Sample concentration (μg/mL)	**Melanin content (MC) (%)[a]**	**Cell viability (CV) (%)**
Control	-	100±5.3	100±2.7
Arbutin	100	55.6±3.1 **	95.0±3.2
OMW	80 [+]	84.1±4.6 **	95.0±3.9
Fruit pulp	80	84.7±2.0**	93.9±2.1
Seeds	160 [+]	89.4±1.7	92.7±3.8
Leaves (May)	80	31.8±1.9 **	98.6±1.4
Leaves (Oct.)	20	80.7±2.9 **	101±2.3
Stems (May)	80	61.2±2.4 **	103±0.5
Stems (Oct.)	40	67.5±2.8 **	97.2±0.8
Flowers	80	67.0±1.2 **	97.8±3.8
Oleuropein	350	58.4±0.3 **	97.8±0.3

The relative activity values (mean±SD) were normalized to the control (n=3). Significant difference between each tested group and the control group was determined using Dunnett's multiple post hoc test (*: $p<0.05$, ** : $p<0.01$) when the one-way ANOVA was significant ([a] : $p<0.01$).

[+] : The non-cytotoxic concentration which was equal to the maximum solubility.

(b)

	B16 melanoma		
	Water extract		
	Sample concentration (μg/mL)	Melanin content (MC) (%)	Cell viability (CV) (%)[a]
Control	-	100±6.1	100±3.1
Arbutin	100	59.2±2.3	89.5±2.9 **
OMW	160 [+]	98.2±7.6	105±1.9
Fruit pulp	160 [+]	101±3.8	101±4.8
Seeds	160 [+]	81.8±0.4	95.4±3.3
Leaves (May)	160 [+]	98.9±4.1	92.9±4.4
Leaves (Oct.)	160 [+]	95.0±2.1	101±1.8
Stems (May)	160 [+]	106±6.3	103±2.3 **
Stems (Oct.)	320 [+]	98.0±5.1	105±3.7
Flowers	40 [+]	105±14	90.0±1.8

The relative activity values (mean±SD) were normalized to the control (n=3). Significant difference between each tested group and the control group was determined using Dunnett's multiple post hoc test (*: $p<0.05$, ** : $p<0.01$) when the one-way ANOVA was significant ([a] : $p<0.01$).

[+] : The non-cytotoxic concentration was equal to the maximum solubility.

2-8. Collagen-production-promoting activity

Fibroblasts produce collagen and hyaluronic acid in extracellular matrix to form dermis, which is an elastic layer of the skin. However, the production of collagen and hyaluronic acid diminishes at more advanced age, which causes wrinkles and sagging. The assay was performed to screen for promoters of collagen production of adult dermal fibroblasts.

NHDF-Ad was seeded on 96-well plates (2×10^4 cells/well) 24 h before the treatment. The medium was replaced with a mixture of 0.5 μL of DMSO solution of EtOH extract and 100 μL of DMEM supplemented with 0.5% FBS. After 72-h cultivation, the amount of collagen in the medium was measured using a human collagen type I ELISA kit. The cells remaining in the 96-well plate were subjected to an MTT assay. The solvent used for dissolving the sample was used as a control, and ascorbic acid (17.6 μg/mL, 100 μM) was used as a positive control.

Table 7 shows the effects of EtOH extracts and oleuropein on the collagen production of NHDF-Ad (CP) and CV. To express CP and CV, each control value was set at 100%. Ascorbic acid, a positive control, increased CP (487%) and had no effect on CV (107%). Of the samples, fruit pulp increased CP the most (427%), followed by leaves (May), stems (May), OMW, leaves (Oct.), stems (Oct.), and seeds. Oleuropein showed no effect on CP (118%). Of the effective samples, leaves (May), fruit pulp, and stems (Oct.) increased CV (145%, 137%, and 130%, respectively), although ascorbic acid did not. Ascorbic acid is a cofactor of procollagen-proline 4-dioxygenase, which is an enzyme necessary for collagen production. Fe (III) ion, which is also a cofactor of the enzyme, is reduced by ascorbic acid, and the enzyme is activated to produce

collagen (Dao *et al.*, 2009). Given these results, some compounds other than oleuropein or the synergistic effect of these three extracts should affect substances other than this enzyme.

Wrinkles or sagging of aged skin is a result of a loss of elasticity and stiffness in the skin due to the reduction of the dermal extracellular matrix (ECM), e.g., collagen, elastin, and hyaluronic acid (Decorps *et al*., 2014). Collagen production by dermal fibroblasts decreases as fibroblasts age (McGrath *et al*., 2012). Also, fibroblast proliferation decreases as they age. In the present results, EtOH extracts of olive by-products promoted not only the CP but also the CV of aged fibroblasts. Further studies on EtOH extracts of fruit pulp and leaves are needed to determine the mechanism.

Table 7 The effect of EtOH extracts of OMW and each part of the olive on collagen production of NHDF-Ad and cell viability.

	NHDF-Ad cell		
	EtOH extract		
	Sample concentration (μg/mL)	**Collagen production (CP) (%)[a]**	**Cell viability (CV) (%)[a]**
Control	-	100±36	100±15
Ascorbic acid	17.6	483±38 **	107±0.52
OMW	400 [+]	324±60 **	122±3.5
Fruit pulp	400 [+]	427±11 **	137±1.3 *
Seeds	400 [+]	163±0 *	93.2±7.6
Leaves (May)	100 [+]	364±51 **	145±6.4 **
Leaves (Oct.)	100 [+]	279±27 **	122±3.7
Stems (May)	100 [+]	352±27 **	97.3±3.6
Stems (Oct.)	100 [+]	275±39 **	130±4.8 *
Flowers	50 [+]	124±28	152±6.8 **
Oleuropein	432	118±13	104±0.7

The relative activity values (mean±SD) were normalized to the control (n=3). Significant difference between each tested group and the control group was determined using Dunnett's multiple post hoc test (*: $p<0.05$, ** : $p<0.01$) when the one-way ANOVA was significant ([a] : $p<0.01$).

[+] : The non-cytotoxic concentration was equal to the maximum solubility.

2-9. Anti-allergic activity

Versatile immune cells are intricately orchestrated in Type I allergy like food allergy, hay fever and AD. To reduce the allergic reaction, it is effective to inhibit the starting reaction which stimulates many cells. Granule release (degranulation) from basophil is one of the major starting reactions, which occurs when basophil recognizes invasion of antigen. The assay described previously (Mira *et al*., 2013) was performed with some modifications to estimate the effect of the samples on degranulation of basophil. A colorimetric assay using ß-hexosaminidase activity was performed to determine the amount of granules released from basophil.

Rat basophilic leukemia cells, RBL-2H3, which are a tumor analog of basophil, were seeded on 96-well plates (5×10^4 cells/well), 24 h before the treatments. First, the cells were treated with 0.5 μg/mL anti-DNP (dinitrophenol) mouse IgE. After 24-h incubation, the medium was replaced with 100 μL of Tyrode's buffer (130 mM NaCl, 5 mM KCl, 1.4 mM $CaCl_2$, 1 mM $MgCl_2 \cdot 6H_2O$, 10 mM HEPES, 5.6 mM glucose, 0.1%(g/v) BSA, pH 7.2), and 0.5 μL of the sample was added to the Tyrode's buffer. After 1-h incubation, 50 μL of the supernatant (S1) was transported to the first new 96-well plate. The Tyrode's buffer containing sample was replaced with 100 μL of fresh Tyrode's buffer containing 5 μg/mL DNP-BSA, which is an antigen of IgE. After 40 min incubation to stimulate the cells to release granules, 50 μL of the supernatant (S2) was transported to the second new 96-well plate. The amount of ß-hexosaminidase in S1 and S2 was measured by colorimetric assay, where the S1 and S2 were mixed with 50 μL of citric acid buffer (pH 4.5) containing 2.0 mM of *p*-nitrophenyl *N*-acetyl-ß-D-glucosaminide and kept in a dark room with shaking at 40 rpm at room

temperature for 3 hr. The absorbance at 405 nm was then measured, after 100 μL of stopping buffer (100 mM of sodium bicarbonate, pH 10) was added. The rates of granule released in S1 and S2 were estimated as G1 and G2, correspondently. The equations are as follows.

$$G1 = \frac{Abs405_{S1\ test} - Abs405_{S1\ BL}}{Abs405_{S2\ cont.} - Abs405_{S2\ BL}} \times 100$$

$$G2 = \frac{Abs405_{S2\ test} - Abs405_{S2\ BL}}{Abs405_{S2\ cont.} - Abs405_{S2\ BL}} \times 100$$

where $Abs405_{S1\ test}$: the absorbance at 405 nm of the reaction solution using S1 in the test well, where EMEM media was replaced with Tyrode's buffer and the cells were treated with 0.5 μL of the sample solution for 1 h. $Abs405_{S2\ test}$: the absorbance at 405 nm of the reaction solution using S2 in the test well, where after S1 of the test well was taken, Tyrode's buffer containing sample was replaced with Tyrode's buffer containing DNP-BSA. S2 in the test well is the supernatant taken after the cells were stimulated with DNP-BSA for 40 min. $Abs405_{S1\ BL}$: the absorbance at 405 nm of the reaction solution using S1 in a blank well, where supernatant taken after the media was replaced with Tyrode's buffer and the cells were treated with 0.5 μL of the solvent used for dissolving the sample (DMSO or distilled water) for 1 h. $Abs405_{S2\ BL}$: the absorbance at 405 nm of the reaction solution using S2 in a blank well, where after S1 of a blank well was taken, Tyrode's buffer containing the solvent was replaced with fresh Tyrode's buffer (DNP-BSA was not added). S2 in a blank well is supernatant taken after the cells were just incubated in fresh Tyrode's buffer for 40 min. $Abs405_{S2\ cont.}$: the absorbance at 405 nm of the reaction solution using S2 in a control well, where firstly the media was

replaced with Tyrode's buffer and the cells were treated with 0.5 μL of the solvent used for dissolving the sample for 1 h. Secondly, Tyrode's buffer containing the solvent was replaced with Tyrode's buffer containing DNP-BSA. S2 in a control well is supernatant taken after the cells were stimulated with DNP-BSA for 40 min.

The CV was measured using an MTT assay after 48-h cultivation period after sample treatment for 1 h. The solvent of the sample was used as a control, and quercetin dehydrate (final concentration: 3.4 μg/mL, 10 μM) was used as a positive control.

Table 8 shows the effects of EtOH extracts, oleuropein, and water extracts on G1, G2, and CV in RBL-2H3 cells. RBL-2H3 cells were treated with the sample for 1 h, and after the Tyrode's buffer was changed, the cells were stimulated by DNP-BSA for 40 min. In this experimental procedure, the amount of granules released from RBL-2H3 cells was measured at two different stages: first, at the end point of the sample treatment (value G1); and second, at the end point of the treatment with DNP-BSA (value G2). G1 and G2 are the relative rate (%) of released granules versus the G2 value of the control. The G1 values of the water extracts of leaves (May and Oct.) and stems (May) increased significantly (183%, 139% and 175%, respectively). These results indicate that the water extracts stimulated the cells to release granules. At the second stage, the cells were stimulated by DNP-BSA to release granules following the sample treatment. Quercetin dihydrate, a positive control, successfully inhibited the release of granules and reduced the G2 value (to 64.6% and 79.0%, respectively). Also, the G2 values of the EtOH extract of OMW and the water extracts of OMW, flowers, leaves (May and Oct.) and stems (May) decreased significantly (to 56.5%, 62.4%, 61.1%, 29.3%, 37.4% and 21.2%, respectively). Oleuropein showed no activity. On the other hand, according

to the G2 values, the water extracts of leaves (May and Oct.) and stems (May) inhibited granule release at the second stage, however, these water extracts stimulated granule release at the first stage. The mechanism of this contradictory phenomenon has not been clarified; however, it is speculated that those water extracts acted ad stimulators of granule release and let RBL-2H3 cells run out of ready-to-release granules at the first stage, and that is why RBL-2H3 cells did not release many granules at the second stage. Considering these results, the EtOH extract of OMW and the water extracts of flowers and OMW were considered as inhibitors and the water extracts of leaves (May and Oct.) and stems (May) were considered as stimulators of granule release. A basophil releases granules when IgEs on the surface of the basophil recognize an antigen. The granules contain inflammatory mediators like histamine and cytokines. Released granules induce the immediate inflammatory reaction of type I allergies such as hay fever and atopy (Ikawati *et al*., 2001). Therefore, substances that inhibit the release of granules induced by antigens have the potential to be effective treatments for type I allergies.

Here, the EtOH extract of OMW was the only one extract which showed the anti-allergic activity. The biological active compound in OMW might be specific to OMW. The malaxation process during olive extraction changes the component in the fruit paste. OMW has a potential to produce specific functional compounds.

Table 8 The effect of (a) EtOH extracts and (b) water extracts of OMW and each part of the olive on granule release from RBL-2H3 cells and cell viability.

(a)

	RBL-2H3 cell			
	EtOH extract			
	Sample concentration (μg/mL)	Granule release (%)		Cell viability (CV) (%)[a]
		G1[a]	G2[a]	
Control	-	23.8±3.5	100±7.6	100±9.4
Quercetin dihydrate	3.4	60.4±6.4 **	64.6±19 *	106±6.6
OMW	400	60.4±5.9 **	56.5±12 **	100±1.6
Fruit pulp	400	56.5±5.2 **	83.1±9.7	108±1.6
Seeds	400	63.8±25 **	83.5±15	110±0.5
Leaves (May)	50	36.9±2.4	115±15	106±6.3
Leaves (Oct.)	50	46.2±10	100±2.9	115±1.8 **
Stems (May)	100	51.9±8.3 *	149±22 *	103±4.7
Stems (Oct.)	100	55.8±2.4 **	113±17	109±2.0
Flowers	50	45.4±10	137±12 *	107±1.9
Oleuropein	350	5.6±2.0	97.2±7.2	100±2.7

The relative activity values (mean±SD) were normalized to the control (n=3). Significant difference between each tested group and the control group was determined using Dunnett's multiple post hoc test (*: $p<0.05$, ** : $p<0.01$) when the one-way ANOVA was significant ([a] : $p<0.01$).

[+] : The non-cytotoxic concentration was equal to the maximum solubility.

G1, G2: the relative amounts of released granules versus control of G2.

Table 8 (b)

RBL-2H3 cell				
	Water extract			
	Sample concentration (μg/mL)	Granule release (%)		Cell viability (CV) (%)[a]
		G1[a]	G2[a]	
Control	-	51.0±7.0	100±16	100±4.4
Quercetin dihydrate	3.4	47.8±8.4	79.0±7.4	105±2.2
OMW	800 [+]	74.7±4.8	62.4±2.2 **	111±2.2 **
Fruit pulp	800 [+]	84.5±33	73.7±15	108±3.3 *
Seeds	400	60.3±7.5	95.6±8.1	109±2.6 *
Leaves (May)	400 [+]	183±36 **	29.3±23 **	112±2.2 **
Leaves (Oct.)	400 [+]	139±14 **	37.4±4.3 **	111±2.3 **
Stems (May)	800 [+]	175±17 **	21.2±5.6 **	108±1.0 *
Stems (Oct.)	800 [+]	52.3±1.7	60.7±38	109±0.9 **
Flowers	200 [+]	89.7±4.7	61.1±10 **	109±5.5 **

The relative activity values (mean±SD) were normalized to the control (n=3). Significant difference between each tested group and the control group was determined using Dunnett's multiple post hoc test (*: $p<0.05$, ** : $p<0.01$) when the one-way ANOVA was significant ([a] : $p<0.01$).

[+] : The non-cytotoxic concentration was equal to the maximum solubility.

G1, G2: the relative amounts of released granules versus control of G2.

2-10. Keratinocyte stimulating activity

Keratinocytes construct the multi-layered epidermis of the skin, which plays

an important role as an intact water proof barrier. Keratinocyte proliferates at the basal layer of epidermis and correctly differentiates into 3 different stages as it is pushed up to outer layer of epidermis (Watt, 1989). Though the cause of psoriasis or AD varies, a symptom of hyperproliferation of keratinocytes and thickening of epidermis is generally seen. In that skin, differentiation of keratinocytes is also not completed (Julia, 2013).

It is well known that differentiation of keratinocyte is controlled by the concentration of extracellular calcium ion (Ca^{2+}). For example, cultured keratinocytes differentiate only in the medium with high concentration of Ca^{2+}, and concentration gradient of Ca^{2+} is formed in intact epidermis with high concentration in the outer layer. The concentration gradient of Ca^{2+} disappears in aged skin or imperfect skin like AD skin (Denda *et al.*, 2003). Also, Ca^{2+} plays an important role in the intracellular signaling. For example, keratinocytes use intracellular Ca^{2+} signal to order to recover a wounded area. The fact that several Ca^{2+} channels which relates to sense of touch are common in terminal nerve cell and keratinocyte also supports the importance of Ca^{2+} signal in keratinocyte (Tsutsumi *et al*., 2013).

Basing on the current knowledge about the function of keratinocytes, it is the most important role for keratinocyte to form an intact epidermis. Here, the effect of the extracts of the olive was determined by two *in vitro* methods. First, the effect of the extracts on transcription of Silent information regulator factor 2 related enzyme 1 (SIRT1) was evaluated. The recent research stated that SIRT1, which is now famous as longevity protein, inhibits proliferation and induce differentiation of keratinocytes, and upregulation of SIRT1 is expected to keep balance of proliferation and differentiation in the thickening epidermis (Wu *et al.* 2014). Because of this, the amount of transcription

of *sirt1* was measured using a reporter assay and RT-PCR experiment. Second, the stimulating effect of the EtOH extract of OMW on Ca^{2+} signal transduction was evaluated using a Ca^{2+} probe, fluo-4.

2-10-1. SIRT1 gene stimulation activity

Reporter assay

First, the activity of the extracts was evaluated by a reporter assay. A human keratinocyte cell line, HaCaT, was transfected with a retro viral vector including SIRT1 promotor region followed by enhanced green fluorescent protein (EGFP). The HaCaT SIRT1p-EGFP cell line was maintained in DMEM supplemented with 10% FBS. The cells were seeded on 96-well black plate at 5×10^3 cells/well and cultured for 24 h. The cells were treated with DMSO solution of either one of the extract or with only DMSO as a control (0.5 μg/well, n=3) for 24 h. The cells were then fixed with 8% paraformaldehyde solution and its nucleus was died with Hoechst for determination of the expressed amount of EGFP per cell. The reagent for each step was prepared freshly. Paraformaldehyde was dissolved in PBS (0.08 g/mL) with NaOH (0.01 N) in a hot water bath at 60 ˚C. An aliquot of 100 μL of paraformaldehyde solution was added to the medium in each well and the well plate was kept at room temperature for 10 min. The wells were emptied with aspirator and washed with 200 μL of PBS for three times. The cells were then dyed with PBS solution of Hoechst33342 (1 μg/mL) at room temperature in a dark place for 30 min. The wells were washed again with PBS for three times and filled with 120 μL of PBS. The fluorescence of EGFP and Hoechst were photographed with an imaging cytometer, IN Cell Analyzer 1000, with the wavelength at Ex: 488 nm and Em: 507 nm for EGFP and at Ex: 360 nm and Em: 460 nm for

Hoechst33342. The average of fluorescent intensity of EGFP in a cell was calculated by a cell image analysis software, IN Cell Analyzer Workstation. Resveratrol was used as a positive control. The data were shown as percentage versus control.

Table 9 shows the promotor activities after treated with each extract or oleuropein for 24 h. Resveratrol activated SIRT1 promotor to 123.2% or 140.6%. The EtOH extract of OMW as well as the EtOH extract of stems (May), stems (Oct.), and fruit pulp and water extract of fruit pulp were also significantly active (106.1%, 109.2%, 112.6%, 107.4% and 105.9%, respectively), but their activity was weaker than that of resveratrol.

Table 9 SIRT1 promotor activity in HaCaT cell measured by reporter assay. HaCaT SIRT1p-EGFP was treated with (a) EtOH extracts and (b) water extracts of OMW or each part of the olive for 24 h.

(a)

	EtOH extract	
	Sample concentration (μg/mL)	**Activity (%)**
Control	-	100±2.0
Resveratrol	2.3	123.2±1.1 **
OMW	200	106.1±1.1 **
Fruit pulp	200	107.4±0.7 **
Seeds	400 +	105.1±2.6
Leaves (May)	25	98.6±2.4
Leaves (Oct.)	25	100.1±1.4
Stems (May)	100 +	109.2±1.3 **
Stems (Oct.)	100 +	112.6±1.8 **
Flowers	25	96.4±0.7 *
Oleuropein	24.4	98.0±2.6

(b)

	Water extract	
	Sample concentration (µg/mL)	**Activity (%)**
Control	-	100±2.3
Resveratrol	2.3	140.6±3.9 **
OMW	800 +	104.2±2.8
Fruit pulp	800 +	105.9±1.7 *
Seeds	400 +	103.6±3.8
Leaves (May)	200	102.8±4.1
Leaves (Oct.)	400 +	99.6±6.5
Stems (May)	400 +	106.5±4.7
Stems (Oct.)	800 +	103.0±1.0

RT-PCR experiment

The promotor activation of the EtOH extract of OMW was confirmed by RT-PCR for continuous 4 days. The amount of mRNA of SIRT1 in HaCaT cell was monitored every 24 h from day 2 to day 5 of the sample treatment period. HaCaT cells were maintained in DMEM supplemented with 10% FBS. The cells were suspended in DMEM medium (10% FBS) at 2×10^4 cells/mL and 5 mL of the cell suspension was dispensed in a 5-cm culture dish and pre-cultured for 24 h. Four culture dishes were prepared for each sample and used for the experiment. An aliquot of 5 μL of DMSO solution of either one of samples or only DMSO was added to the medium of all the culture dishes in the first and second day. From the third day, one dish was taken from each treatment group and the sample was added again to the remaining culture dishes. The dishes taken from each treatment group were used for collecting cell lysate, which was kept in -20 ˚C until it was used for total RNA purification. After all the cells were harvested, the cell lysates were melted and total RNA was purified using High Pure RNA isolation Kit following manufacturer's instruction manual. Reverse transcription was performed using ReverTra Ace kit with Random Primers for RT-PCR. The primers of ß-actin and SIRT1 were used for RT-PCR. Resveratrol, rolipram and fisetin were used as a positive control. ß-Actin was used as a house keeping gene and the data were shown as percentage versus control.

Table 10 shows the results of RT-PCR experiment. The value of SIRT1/ß-actin increased around 1.2 times, when the cells were treated with the EtOH extract of OMW for 120 h. The On keratinocyte, activation of SIRT1 by natural phenolic compound inhibited cell hyperproliferation, which is a symptom of psoriasis

and AD (Wu *et al.* 2014). SIRT1, a member of mammalian homologues of sirtuins, is one of the most famous nicotinamide adenine dinucleotide (NAD^+)-dependent deacetylase. Upregulation of SIRT1 has been reported to protect mice from aging-related phenotypes, including diabetes (Banks *et al.* 2008, Brodone *et al.* 2007, Pfluger *et al.* 2008), cancer (Herranz *et al.* 2010), Alzheimer's diseases (Donmez *et al*.2010), and cardiovascular diseases (Lina *et al.* 2015), and as a result the life span of individual is elongated. Because the benefit of upregulation of SIRT1 in keratinocyte has not been fully elucidated, the whole effect of the EtOH extract of OMW on keratinocyte is expected to be determined.

Table 10 The relative value of mRNA of SIRT1 versus control. Three positive compounds and the EtOH extract of OMW were added to the medium of HaCaT every 24 h. Total RNA was collected at 48, 72, 96 and 120 h after the first sample addition. ß-Actin was used as house keeping gene.

	Conc.	SIRT1/ß-actin (%)			
	(μg/mL)	48 h	72 h	96 h	120 h
Control	-	100±5.6	100±11.9	100±12.0	100±6.4
Resveratrol	1.1	107.4±1.4	115.1±7.6	173.6±14.1 **	172.9±8.6 **
Rolipram	0.72	87.8±8.2	80.0±1.2	114.1±9.0	127.3±9.0 *
Fisetin	2.8	92.1±3.2	80.9±0.7	134.4±0.5 **	214.5±26.5 **
OMW (EtOH)	100	102.8±4.0	82.0±9.6	121.2±10.3	124.0±2.7 **

2-10-2. Calcium ion signal stimulation activity

The concentration of Ca^{2+} ($[Ca^{2+}]$) in HaCaT cell was monitored using an imaging cytometer, IN Cell analyzer 1000. To monitor intracellular $[Ca^{2+}]$ soon after the sample addition, the samples needed to be added with an auto sampler furnished in IN Cell analyzer 1000. Because repeatability was not obtained at first, the washing method for the auto sampler was optimized after several trials. Then, the effect of each extract was estimated.

Cell culturing: HaCaT cell was sustained in 10 mL of DMEM medium supplemented with 10% FBS for one week at 37 °C under a 5% CO_2 atmosphere. The cells were passaged every third or fourth day to a new dish (1×10^5 cells/mL). Then the medium was removed with an aspirator and the dish was rinsed once with 5 mL of PBS. The cells were then treated with 1 mL of 0.25% trypsin containing EDTA for around 10 seconds and the trypsin solution was removed. After incubation for 8 minutes, the HaCaT cells were detached from the dish by tapping and suspended in 10 mL of DMEM (10% FBS). The cell suspension was put in 6 wells of a 96-well black plate (2×10^5 cells/mL, 100 μL/well); then the cells were cultured in an incubator for 2 days until confluence.

Preparation of cell plate and sample plate: Cell plates containing dyed cells and a sample plate containing the sample dissolved in medium were prepared for measurement of intracellular $[Ca^{2+}]$ in HaCaT cells. After incubation for 2 days, the cells were dyed with Hoechst33342 and fluo-4 reagent. First, reagents were prepared just before use. Hoechst33342 (1 mg/mL, Dojindo) was diluted for 500 times in DMEM (FBS was not added), and fluo-4 reagent was prepared following the manufacturer's

instruction and mixed with the same volume of DMEM. Second, the supernatant of the cell plate was removed and 100 μL of the Hoechst33342 solution was added to each well. The cell plate was incubated at room temperature in a dark place for 30 minutes. The supernatant was removed and the wells were washed twice with 200 μL of PBS to finish dying. Then, 100 μL of the fluo-4 mixture in DMEM was added to each well and incubated for 1 hour in an incubator. This plate is called the "cell plate" in this article. All the steps to change the supernatant were done quickly, so that the cells at the bottom of the well would not be dried up.

After incubation with fluo-4, the cells were exposed to each sample in the IN Cell analyzer 1000 for 180 seconds, and intracellular [Ca^{2+}] was monitored constantly during this period. The sample was transferred from the sample plate to the cell plate using auto sampler. The sample plate was prepared using a 96-well clear plate. First, EtOH extract of olive milled waste (OMW, containing oil) was dissolved in DMSO at 60, 30, 15, 7.5, 3.8 mg/mL. Then, 1 μL of the sample solution and 200 μL of DMEM (10% FBS) was mixed in 6 wells of a 96-well clear plate. The control medium was 200 μL of DMEM (10% FBS) containing DMSO (0.5% (v/v)).

Washing auto sampler: The IN Cell analyzer 1000 is equipped with one auto sampler and one rinsing pump for supplying water to the auto sampler. However, oily samples or hydrophobic compounds dissolved in water-based solvent are possibly absorbed onto the auto sampler surface and are difficult to remove by rinsing with water. This causes contamination and unreliable results. Accordingly, it was tried to rinse the auto sampler with both 50% ethanol (EtOH) and water. In order to make the system wash the auto sampler with 50% EtOH and rinse it with water, two 96-well plates were

prepared: one plate containing 200 μL of 50% EtOH in 4 wells (the "supply plate") and another empty plate (the "receiving plate"). These two plates were set in the IN Cell analyzer 1000. First, the auto sampler pumped up to 50 μL of 50% EtOH from the supply plate and discharged it to the receiving plate. After the motion of pumping up and discharging, the furnished camera formally took some pictures for 20 seconds. Then the auto sampler was rinsed with 10 mL of ultrapure water supplied from the rinsing pump. These steps were repeated for 4 times.

Measurement of intracellular [Ca^{2+}] using an imaging cytometer: The cell plate and the sample plate were put on the dock plate of IN Cell analyzer 1000. Then, the system of the auto sampler was operated to absorb 50 μL from the sample plate, and to discharge 50 μL at the rate of 80 μL/sec to the supernatant of the cell plate at 0 seconds of measurement. The auto sampler was rinsed with 10 mL of water supplied from the rinsing pump before each new sample was added. The measurement of fluorescence lasted 180 seconds. During the measurement, a camera equipped with the IN Cell analyzer 1000 took pictures of an area at 0 second and every 5 second from 15 to 180 second (Ex: 360 nm and Em: 460 nm for Hoechst33342, Ex: 480 nm and Em: 535 nm for fluo-4). The sequence of the sample addition, image capturing and rinsing the auto sampler was conducted well by well.

The images taken at every time point were analyzed with the software, IN Cell analyzer Workstation 3.7. The software detected the intensity of fluorescence emitted from the Hoechst33342 and fluo-4 independently, and calculated the number of nuclei in the area and the product of the fluorescence area multiplied by the fluorescence intensity, indicating the amount of intracellular Ca^{2+}. The intracellular

[Ca^{2+}] was calculated as follows:

Intracellular [Ca^{2+}] = [Concentration of Ca^{2+} in the area] / [Number of nucleus].

In the result figures, [Ca^{2+}] is shown to start from 0 at 0 seconds.

Results and discussions: First, the methods using IN Cell Analyzer 1000 was optimized to obtain repeatable data of the intracellular [Ca^{2+}] of keratinocyte. When the fluorescent probe is applied to real-time quantitative observation, it is effective to use image analysis on fluorescent images of dyed cells photographed with a fluorescence microscope or imaging cytometer (Guying *et al.*, 2014; Tao *et al.*, 2006). For this purpose, a built-in auto sampler should be utilized, so that the measurement can be started soon after adding the sample.

The IN Cell analyzer 1000 is furnished with one stainless-steel auto sampler and one washing line for it. At first, ultrapure water was connected to the equipped washing line; however, the results obtained were not reliable (Fig. 2 A and B). It was suspected that some of the compounds were carried over to control wells, because some samples have low solubility in water and can remain in the auto sampler.. Accordingly, the washing method of the auto sampler was optimized to supply two kinds of washing solvent. The first solvent, 50% EtOH, was supplied in the same way as the samples, and the second solvent, water was supplied with the furnished pump. Specifically, the first solvent was placed in a few wells of the supply plate and pumped up and drained out to the receiving plate. Then, every time after the transfer of the first solvent, 10 mL of the second solvent was supplied to rinse the auto sampler. The 50% EtOH was better than 0.1 M sodium hydroxide (NaOH) and 99.5% EtOH as the first solvent.

Second, the activity of the EtOH extract of OMW was confirmed by the

optimized method. The experiment was scheduled as shown in Fig. 2. First, as a control before washing the auto sampler correctly, a sample plate with control medium was prepared. Then, 50 μL was transferred to the cell plate and intracellular [Ca^{2+}] was monitored (n=6). Second, the auto sampler was washed with 50% EtOH. Third, to figure out the difference before and after the washing, 50 μL of control medium was added to the cell plate and [Ca^{2+}] was monitored in the same manner as before washing (n=6). Finally, a sample plate with DMEM containing 6 different concentrations of OMW was prepared. Then 50 μL was transferred from the sample plate to the cell plate. The results shown in Fig. 3 indicate each time-course of intracellular [Ca^{2+}] (A, C and E) and maximum plots of the line (B, D and F). Comparing the time-course lines or maximum plots of the control before (Fig. 3 A and B) and after washing (Fig. 3 C and D), we can see that the dispersion of the time-course lines before washing was minimized after washing, and the time-course lines went on almost the same path and the value of the maximum plot was stable. Also, when the active OMW sample was added at concentrations from 0 μg/mL to 100 μg/mL, the intracellular [Ca^{2+}] increased dose-dependently (Fig. 3 E and F), indicating that the EtOH extract of OMW has some effect on keratinocyte.

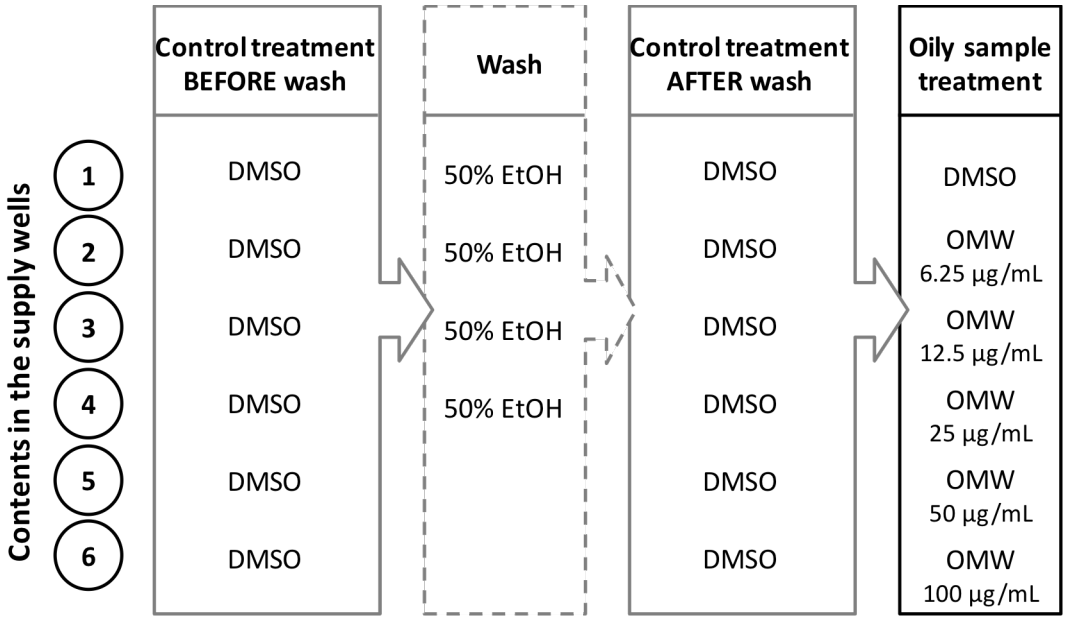

Fig. 2 The experimental schedule of measurement of intracellular [Ca^{2+}] in HaCaT cell.

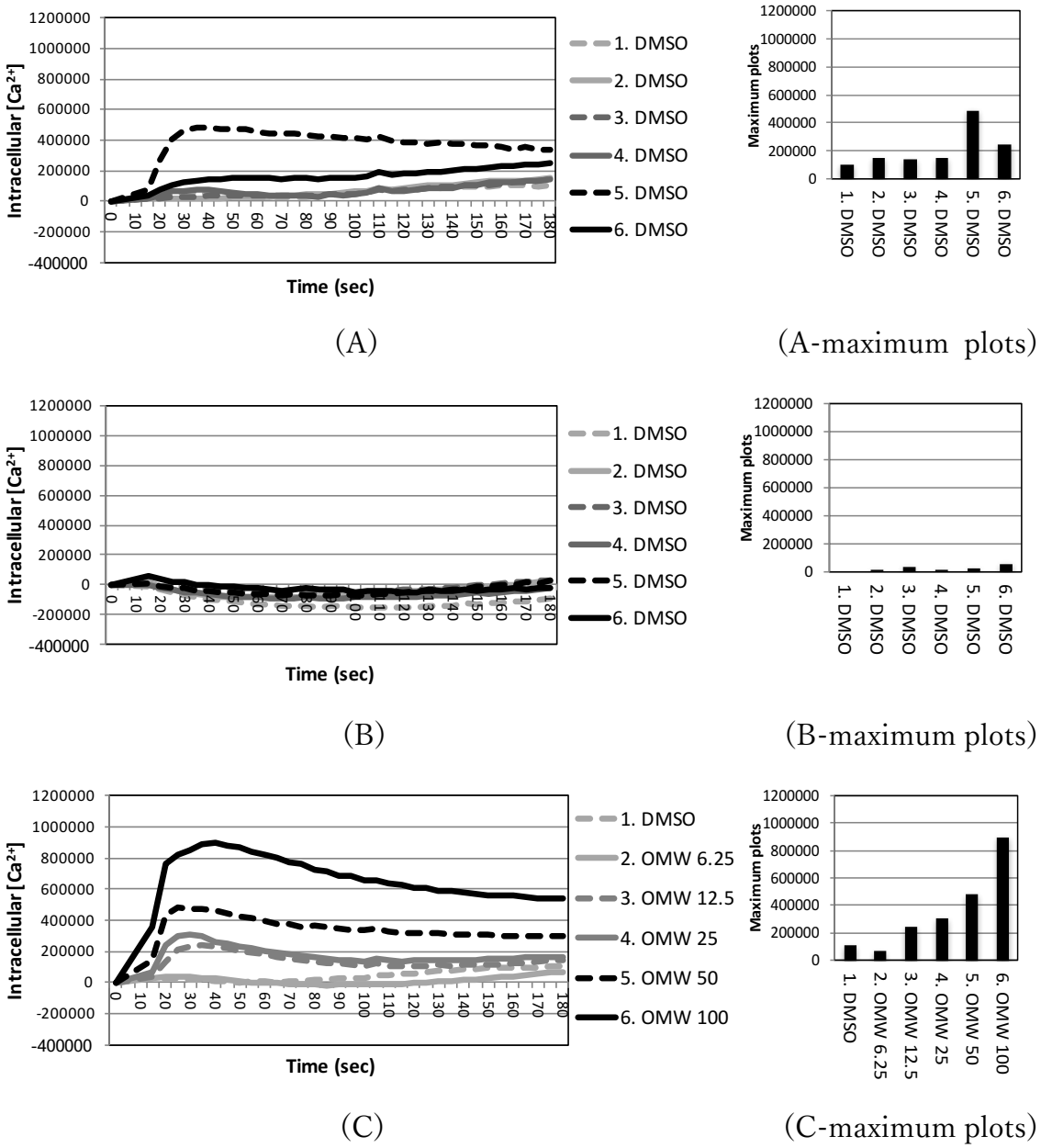

Fig. 3 Results of the Ca^{2+} assay on HaCaT cells before and after washing the auto sampler. (A) DMSO was added before washing the auto sampler. (B) DMSO was added after washing the auto sampler. The data became stable and the washing method was confirmed. (C) Then, the EtOH extract of OMW was added at 5 different concentrations (μg/mL) using the confirmed washing method.

2-11. Short summery

In this chapter, several *in vitro* assays were conducted to evaluate and compare the biological activities of the extracts of OMW with the other extracts. EtOH extracts showed relatively higher activity in each assay than the corresponding water extracts. Comparing the biological activities of the EtOH extract of OMW with that of the EtOH extracts of each part of the olive, the EtOH extract of OMW specifically showed anti-allergic activity, while the EtOH extracts of fruit pulp and seeds were not active. During olive oil extraction where the fruits are crashed and mixed well, several enzymatic reactions oxidize, glucosidate or hydrolyze the extractives. It is possible that some compounds in the olive fruits were transformed to the active forms and resulted in the different activity. In the previous report, a secoiridoid and luteolin were isolated as anti-allergy active compounds from olive pomace that was prepared using a hand mixer from fruits of the Mission cultivar grown in Japan (Sato *et al*., 2014). However, little has been reported about the anti-allergic compounds in OMW.

Also, in the keratinocyte stimulating assay, the EtOH extract of OMW stimulated the transcription of SIRT1 gene and transduction of intracellular Ca^{2+} signaling. To elucidate the influence of the stimulation, it is important to know which compound contributes the stimulation. In the next Chapter, the biological active compounds for anti-allergy are discussed.

Chapter 3: Anti-allergic compounds isolated from the EtOH extract of OMW

3-1. Introduction

Although basophils compose less than 1% of peripheral blood leucocytes, recent findings indicate that basophils play important roles in a wide variety of immune regulation functions and disorders such as immediate hypersensitivity reactions, late-phase hypersensitivity reactions, autoimmunity, and cancers (Cromheecke et al. 2014; Harvima et al. 2014; Siracusa et al. 2013). Basophils are involved in the orchestration of immune responses by releasing histamine or several cytokines mediated by IgE or other cytokines. The degranulation of basophils mediated by IgE cross-linking is one of the main triggers of immediate hypersensitivity reactions such as anaphylaxis and allergy to foods, drugs, insects, pollens and so on.

In the previous examinations of the biological active potentials of EtOH extract and water extract of OMW and each part of the olive, it was observed that the degranulation of RBL-2H3 was inhibited only by the EtOH extract of OMW whereas the EtOH extract of fruit pulp or that of seeds showed very weak activity (Kishikawa et al. 2015).

Olive oil and methanol extract of olive waste materials were also reported to have inhibitory activity on degranulation of RBL-2H3. The active compounds of those olive materials were mainly phenolic compounds. For example,

flavonoids such as apigenin and luteolin were shown to be the active compounds for olive oil, and a secoiridoid connected to hydroxytyrosol like 2-hydroxy-3-ethylidene-5-(methoxycarbonyl)-3,4-dihydro-2*H*-pyran-4-acetic acid 2-(3,4-dihydroxyphenyl)ethyl ester (3,4-DHPEA-EA) are reported to be the active compound for olive waste materials (Isoda et al. 2012; Sato et al. 2014). The main triterpenes of OMW were reported to have antitumoral activity, cardioprotective activity, anti-inflammatory activity and antioxidant activity (Sanchez-Quesada et al. 2013).

As a result of the increasing interest in OMW, we chromatographed the EtOH extract of OMW for the present investigation of its anti-allergic compounds, and successfully a new triterpene with anti-allergic activity was isolated. Also some possible substructures of the olive triterpenes that may be involved in the anti-allergic activity are discussed.

3-2. Materials and Methods

3-2-1. Cell line and reagents

The cell line of rat basophilic leukemia (RBL-2H3, Riken Bioresource Center, Ibaraki, Japan) was maintained in 10% FBS (Thermo Fisher Science, Gibco BRL, Tokyo, Japan) in EMEM (Nissui, Tokyo, Japan) in an incubation at 37 ˚C, 5.0% CO_2. Monoclonal anti-dinitrophenyl antibody produced in mouse (IgE anti-DNP) and *p*-nitrophenyl *N*-acetyl-ß-D-glucosaminide were purchased from Sigma-Aldrich (St. Louis, MO) and dinitrophenyl-bovine serum albumin (DNP-BSA) was purchased from Thermo Fisher Scientific, Invitrogen (Tokyo, Japan). 3-(4,5-Dimethylthiazol-2-yl)-2,5-Diphenyltetrazolium Bromide (MTT) reagent was purchased from Tokyo Chemical Industry (Tokyo, Japan). For analysis of fractions or isolated compounds, TLC silica gel 60 F_{254}, methanol-d_4 (CD_3OD) and dimethyl sulfoxide-d_6 (DMSO-d_6) were purchased from Merck (Darmstadt, Germany), Cambridge Isotope Laboratories (Andover, MA) and Sigma-Aldrich (St. Louis, MO), respectively. Wakogel C 200 (silica gel, pore size 7 nm, particle diameter 75-15 μm), *n*-hexane (Hex), ethyl acetate (EtOAc) and methanol (MeOH) were purchased from Wako Pure Chemical Industries (Osaka, Japan) and used for open column chromatography.

3-2-2. Extraction and chromatography

OMW was collected from an olive farm in Nakagawa in Japan's Fukuoka prefecture in October 2013. The fresh OMW was freeze-dried, and then 30 g of the freeze-dried OMW was extracted with 300 mL of EtOH with shaking at 200

rpm in a 500-mL flask for 72 h. This extraction step was repeated until 360.1 g of EtOH extract was obtained from 1.92 kg of freeze-dried OMW in total. The extraction yield was 18.8%.

The EtOH extract of OMW was chromatographed roughly with a silica gel open column (15 cm dia., with 2 kg of silica gel) using the gradient solvent system of Hex, EtOAc and MeOH. The effluent was classified into fractions by monitoring with a thin-layer chromatography (TLC) analysis, detected by irradiating UV light at 254 nm and by spot visualization, in which the TLC plate was sprayed with 5% sulfuric acid/methanol and burned at 100° –180° C. A medium pressure liquid chromatography (MPLC) system (EPCLC, Yamazen, Osaka, Japan) connected with columns of silica gel (particle size 50 μm, 3.0 × 16.5 cm, 37 g) and ODS-SM (particle size 30 μm, 3.0 × 16.5 cm, 40 g) was the second step of fractionation. A preparative high-performance liquid chromatography (HPLC) system (Waters, Milford, MA, USA) connected with an Inertsil ODS column (particle size 5 μm, 20 × 250 mm, GL Science, Tokyo) was used for further purification.

3-2-3. Identification of isolated compounds

We identified the isolated compounds by measuring high-resolution electrospray ionization mass spectrometry (HR-ESI-MS) and nuclear magnetic resonance (NMR) spectroscopy, and the optical rotation of the compounds was evaluated. The HR-ESI-MS results were obtained using a liquid chromatography-ion trap-time of flight-mass spectrometry (LC-IT-TOF-MS)

system (Shimadzu, Kyoto, Japan) equipped with an Inertsil ODS-3 column (particle size 3 μm, 1.5 × 150 mm, GL Science). The solvent system was isocratic, composed of 90% LC grade MeOH containing 0.1% formic acid. The flow rate was set at 0.2 mL/min. The ^{1}H-, ^{13}C-, heteronuclear single quantum coherence (HSQC), heteronuclear multiple bond correlation (HMBC) and nuclear Overhauser effect spectroscopy (NOESY) NMR spectra were obtained on an NMR spectrophotometer (Bruker DRX 600; Bruker Daltonics, Billerica, MA) at room temperature with tetramethylsilane (TMS) as an internal standard of chemical shifts and CD_3OD or DMSO-d_6 as solvents. Optical rotations in MeOH were determined with a polarimeter (DIP-370; Jasco, Tokyo).

3-2-4. Anti-allergic assay

We subjected the triterpenes to an anti-allergic assay to determine their cytotoxicity (CC_{50}, half-minimum cytotoxic concentration and CC_{10}, 10%-minimum cytotoxic concentration) and their effect on the degranulation of RBL-2H3 (IC_{50}, half-minimum inhibitory concentration and IC_{40}, 40%-minimum inhibitory concentration). In this study, we defined 'cytotoxicity' as the characteristic causing a reduction in the cell viability to 90% or lower versus the control, and we defined 'anti-allergic activity' as an inhibitory effect on ß-hexosaminidase release from RBL-2H3 cells without showing cytotoxicity, because a reduction of ß-hexosaminidase release by killing the cell cannot be accepted as anti-allergic activity. We also defined an 'anti-allergic compound' as a compound that shows 50% or 40% inhibition of ß-hexosaminidase release at a

concentration lower than 100 μM without cytotoxicity. The experiment was done as described (Kishikawa et al. 2015) with some modifications.

Cytotoxicity was evaluated by an MTT assay. The RBL-2H3 cells were cultured on a 96-well plate at a density of 5×10^4 cells/well for 36 hr, and treated with a dimethyl sulfoxide (DMSO) solution of either one of the test samples at various concentrations or with only DMSO as a control (0.5 μL/well, n=3). The cytotoxicity was evaluated using MTT assay after 1-hr treatment. Each of the values of CC_{50} and CC_{10} was calculated from the concentrations of two data points interposing cytotoxicity of 50% or 10%, respectively.

For the determination of the IC_{50} and IC_{40} values, the RBL-2H3 cells were cultured on a 96-well plate at 5×10^4 cells/well for 24 hr and with IgE anti-DNP (0.5 μg/mL) for an additional 12 hr. The cells were treated with DMSO solution of the samples at several concentrations lower than the CC_{10} or only DMSO as a control for 1 hr (0.5 μL/well, n=3). The cells were then stimulated in 100 μL of Tyrode's buffer (pH 7.2) containing 5 μg/mL of DNP-BSA for 40 min. Then 50 μL of supernatant was carefully transferred to a new 96-well plate to be mixed with 50 μL of citric acid buffer (pH 4.5) containing 2.0 mM of *p*-nitrophenyl *N*-acetyl-ß-D-glucosaminide. The ß-hexosaminidase reaction occurred in a dark room with shaking at 40 rpm at room temperature for 3 hr. For the determination of the IC_{50} and IC_{40} values, we calculated the inhibition of ß-hexosaminidase release from the absorbance at 405 nm after stopping the reaction with 100 μL of sodium bicarbonate (100 mM, pH 10):

$$\text{Inhibition } (\%) = \left(1 - \frac{Abs405_{comp.} - Abs405_{blank}}{Abs405_{cont.} - Abs405_{blank}}\right) \times 100$$

where $Abs405_{comp.}$ is the absorbance at 405 nm of the test well (DMSO solution: +, DNP-BSA: +), $Abs405_{cont.}$ is the absorbance at 405 nm of a control well (DMSO: +, DNP-BSA: +), and $Abs405_{blank}$ is the absorbance at 405 nm of a blank well (DMSO: +, DNP-BSA: −). Each of the values of IC_{50} and IC_{40} was calculated from the concentrations of two data points interposing the inhibition value of 50% or 40%, respectively. Ursolic acid was used as a positive control, because ursolic acid was reported to inhibit the degranulation of RBL-2H3 cells (Murata et al. 2014), and it has a structure similar to that of the isolated compounds.

3-3. Results

3-3-1. Isolation from EtOH extract of OMW

As a result of silica gel open column chromatography, the EtOH extract of OMW was fractionated into 10 fractions with detection of effluents by TLC: (SiO_2, Hex/EtOAc 8 : 2, spot visualization) Fr. 1, R*f* 0.63-0.83; Fr. 2, R*f* 0.45-0.55; Fr. 3, R*f* 0.28-0.35; Fr. 4, R*f* 0.13-0.17; (SiO_2, Hex/EtOAc 5 : 5, spot visualization) Fr. 5, R*f* 0.33-0.60; Fr. 6, R*f* 0.10-0.29; (SiO_2, EtOAc/MeOH 7.5 : 2.5, spot visualization) Fr. 7, R*f* 0.36-0.67; Fr. 8, R*f* 0.11-0.40; Fr. 9, R*f* 0.11-0.22; Fr. 10, R*f* <0.02. Fr. 5 and Fr. 6 were subjected to further fractionations, because Fr. 6 showed the highest anti-allergic activity and Fr. 5 showed similar TLC profile with Fr. 6. Fr. 5 (3.5 g) was the fraction eluted out from the open column with the gradient mobile phase Hex : EtOAc = 70 : 30 to 30 : 70 and Fr. 6 (15.5 g) was the fraction eluted with the solvent Hex : EtOAc = 30 : 70 to 10 : 90.

Fr. 5 was chromatographed using MPLC system and preparative HPLC system (Waters Corporation, USA). As a result, Fr. 5 provided compound **1** (15 mg), **2** (20 mg) and **3** (1.5 mg). Fr. 6 was fractionated again with a silica gel open column (ϕ 6 cm, with 0.8 kg of silica gel) by gradient solvent system of Hex, EtOAc and MeOH. In order to obtain better separation, acetic acid was added to the chromatographic solvent at 0.25% (v/v) and the solvent and acetic acid were evaporated soon after collected from the open column. By monitored with TLC, the effluents of Fr. 6 was fractionated into 10 sub fractions: (SiO_2, Hex/EtOAc 5 : 5, spot visualization) Fr. 6-1, R*f* 0.63-0.86; Fr. 6-2, R*f* 0.31-0.70; Fr. 6-3, R*f*

0.23-0.63; Fr. 6-4 to6-9 R*f* 0.08-0.55; Fr. 6-10, R*f* <0.08. Compound 1 was distributed in the sub fractions from Fr. 6-3 to Fr. 6-8 in large amount, some other spots in Fr. 6-3, 6-4 and 6-8 were the target for the further isolation. Fr. 6-3 was the fraction collected from the open column with the mobile phase Hex : EtOAc = 80 : 20 to 75 : 25, Fr. 6-4 was collected with Hex : EtOAc = 70 : 30 and Fr. 6-8 was collected with Hex : EtOAc = 55 : 45 to 50 : 50. With the several times of purification with MPLC and preparative HPLC systems, compound **1** (4.0 mg), **2** (0.8 mg), **4** (0.6 mg), **8** (1.1 mg), **9** (2.0 mg) and **10** (2.2 mg) were isolated from Fr. 6-3 (453 mg), compound **5** (0.4 mg) was obtained from Fr. 6-4 (187 mg), and compound **6** (1.8 mg) and **7** (3.2 mg) was successfully isolated from Fr. 6-8 (2.3 g).

3-3-2. Identification of the isolated compounds

Six of the ten compounds were identified as triterpenes (**1-6**) including one new triterpene, 2α,3β-dihydroxy-11-oxo-18β-olean-12-en-28-oic acid (11-oxo-maslinic acid, **6**) and four of them were identified as phenolic compounds (**7-10**) (Fig. 4).

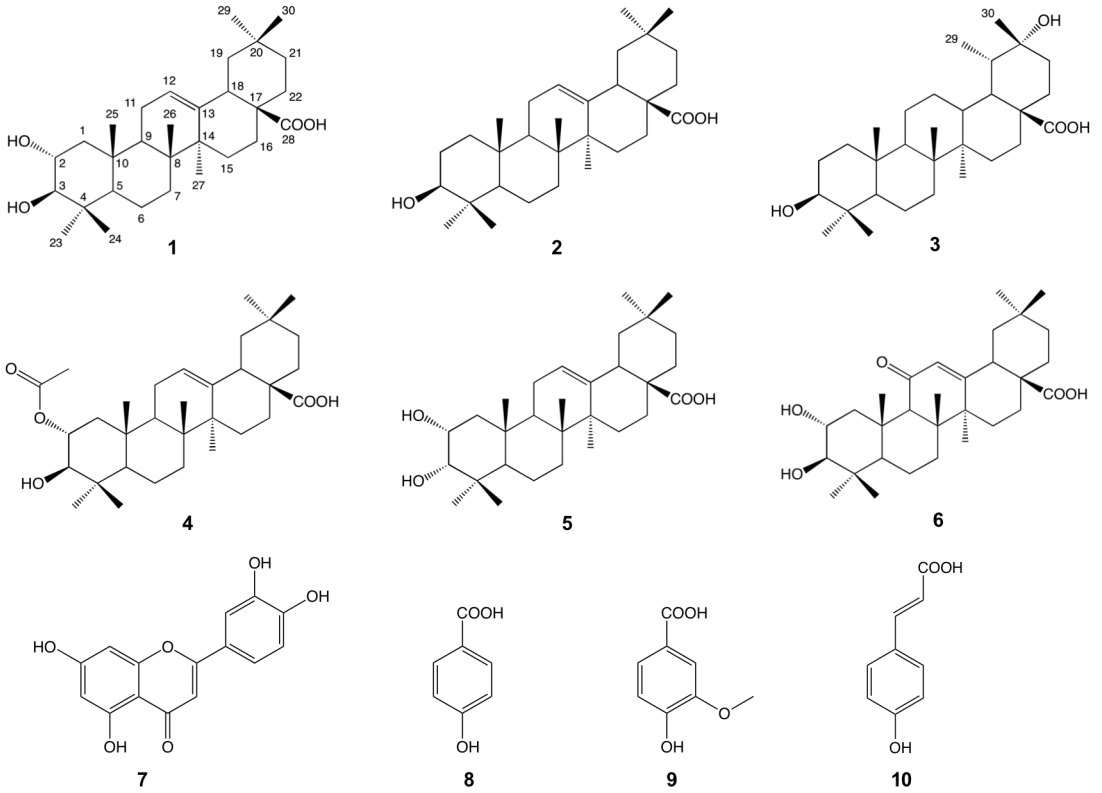

Fig. 4 The structure of ursolic acid and the isolated triterpenes: maslinic acid (**1**), oleanolic acid (**2**), punicanolic acid (**3**), 2-*O*-acetylmaslinic acid (**4**), epimaslinic acid (**5**), 11-oxo-maslinic acid (**6**), luteolin (**7**), *p*-hydroxy benzoic acid (**8**), vanillic acid (**9**) and

Compound **6** was obtained as a yellowish amorphous powder with $[\alpha]^{26}_{D}$ +49.0 (*c* 1.0, MeOH). HR-ESI-MS exhibited a protonated molecular ion peak at *m/z* 487.2911 $[M+H]^+$ and a deprotonated molecular ion peak at *m/z* 485.3356 $[M-H]^-$ in positive and negative ion modes, respectively, indicating a molecular formula of $C_{30}H_{46}O_5$. It showed UV λ_{max} 252 nm (0.1% formic acid in MeOH). The ^{1}H-NMR spectral data was indicative of seven tertiary methyl groups at δ_H 1.46 (H-27), 1.17 (H-25), 1.02 (H-23), 0.98 (H-26), 0.96 (H-30), 0.95 (H-29) and δ_H 0.82 (H-24) together with an olefinic proton at δ_H 5.55 (br s). The methyl protons were correlated through HSQC spectrum to δ_C 24.0, 18.0, 29.3, 19.9, 23.8, 33.0 and δ_C 17.5, respectively. Furthermore, the HSQC experiment showed the correlation of the broad singlet at δ_H 5.55 with δ_C 128.3. These NMR characteristic features suggested compound **3** to be a triterpene possessed an olean-12-ene skeleton (Mahato and Kundu, 1994). The carbon signal at δ_C 128.3 was then placed to C-12 of the skeleton. The ^{13}C-NMR spectrum furthermore revealed carbon signals at δ_C 202.7, 180.9, 128.3, 172.9, 84.2 and δ_C 69.2. With the help of HMBC correlations, the carbon signal at δ_C 202.7 was unambiguously assigned to C-11 of the skeleton based on the correlation observed from δ_H 5.55 (H-12) to δ_C 202.7 and further confirmed from the correlations of δ_H 2.48 (1H, s), assigned to H-9 with δ_C 202.7. The carbon signal at δ_C 180.9 was assigned to a carboxylic group attached to C-28. The quaternary carbon signal at δ_C 172.9 was placed to C-13 of the skeleton. The assignment of δ_C 180.9 to C-28 and δ_C 172.9 to C-13, was evidenced from the long-range correlations observed from δ_H 3.00 (dd, *J*=3.6, 13.8 Hz, H-18)

with the carbon signals at δ_C 180.9, 172.9 together with its correlation to δ_C 128.3 (C-12) and δ_C 43.4 (C-18). The two oxygen-bearing carbons at δ_C 84.2 and δ_C 69.2 were carefully placed to C-3 and C-2 of the olean-12-ene skeleton based on long-range correlations observed from δ_H 3.08 (dd, J=4.2, 12.6 Hz, H-1) with δ_C 84.2 and δ_C 69.2 and by comparison with (Martinez et al., 2013; Rudiyansyah and Garson, 2006; Tanaka et al., 2003) which justified 2α,3β-diol. On the basis of the above discussion, the structure of **6** was established as 2α,3β-dihydroxy-11-oxo-18β-olean-12-en-28-oic acid, which is a new natural product.

The other compounds were identified as maslinic acid (**1**), oleanolic acid (**2**) (Martinez et al. 2013), punicanolic acid (**3**) (Xie et al. 2008), 2-*O*-acetylmaslinic acid (**4**) (Thoison et al. 2004) and epimaslinic acid (**5**) (Wen et al. 2008), luteolin (**7**) (Flamini et al. 2001; Miyazawa et al. 2003), *p*-hydroxy benzoic acid (**8**) (Sengab et al. 2015; Youn et al. 2010), vanillic acid (**9**) (Bollag et al. 1982) and *p*-coumaric acid (**10**) (Ashour et al. 2013) by comparing their spectral data with those reported in the literature. Maslinic acid (**1**) and oleanolic acid (**2**) are known as the main triterpenes in OMW, olive fruits, olive oil and olive leaves. These triterpenes are reported to have a wide variety of biological effects such as anticancer, cardioprotective, anti-inflammatory, antioxidant, anti-HIV, antimicrobial, and hepatoprotective activities (Sanchez-Quesada et al. 2013; Fernandez-Hernandez et al. 2015). Punicanolic acid (**3**), 2-*O*-acetylmaslinic acid (**4**) and epimaslinic acid (**5**) were isolated from the olive plant for the first time in this study. As for 2-*O*-acetylmaslinic acid (**4**),

considering the earlier finding that pectin extracted from the olive mill wastewater was highly acetylated to increase its oil holding capacity (Rubio-Senent et al. 2015), it is apparent that maslinic acid can also exist in OMW as an acetylated form. Maslinic acid (**1**), oleanolic acid (**2**) and epimaslinic acid (**5**) are present in many plants, whereas punicanolic acid (**3**) was isolated from flowers of *Punica granatum* (pomegranate) (Xie et al. 2008) and 2-*O*-acetylmaslinic acid (**4**) was isolated from leaves of the trees *Nothofagus dombeyi* and *N. pumilio* (Thoison et al. 2004). The data used for identification are follows:

Maslinic acid (2α, 3β–Dihydroxyolean-12-en-28-oic acid, **1**)

White amorphous solid: $[\alpha]^{26}_{D}$ +52.2 (*c* 1.0, MeOH): TLC (SiO_2, Hex/EtOAc/MeOH 5 : 5 : 0.1, spot visualization) R*f* 0.29: ^{1}H NMR (600 MHz, CD_3OD) δ_H 5.25 (1H, dd, *J*= Hz, H-12), 3.61 (1H, ddd, *J*=4.8, 9.6, 11.4 Hz, H-2ß), 2.90 (1H, d, *J*=9.6 Hz, H-3α), 2.85 (1H, dd, *J*=4.2, 14.4 Hz, H-18), 2.00 (1H, ddd, *J*= Hz, H-16), 1.16 (3H, s, H-27), 1.01 (3H, s, H-23), 1.00 (3H, s, H-25), 0.94 (3H, s, H-30), 0.91 (3H, s, H-29), 0.81 (3H, s, H-26), 0.81 (3H, s, H-24): for ^{13}C NMR (150 MHz, CD_3OD), see Table1: HR-ESI-MS *m/z* 471.3504 $[M-H]^-$.

Oleanolic acid (3β-hydroxyolean-12-en-28-oic acid, **2**)

White amorphous solid: $[\alpha]^{26}_{D}$ +65.6 (*c* 1.0, MeOH): TLC (SiO_2, Hex/EtOAc/MeOH 5 : 5 : 0.1, spot visualization) R*f* 0.52: ^{1}H NMR (600 MHz, CD_3OD) δ_H 5.24 (1H, dd, *J*= Hz, H-12), 3.14 (1H, dd, *J*=4.2, 9.6, 11.4 Hz,

H-2ß), 2.84 (1H, dd, *J*=4.2, 13.8 Hz, H-18), 2.01 (1H, ddd, *J*=4.2, 13.8, 13.8 Hz, H-16), 1.16 (3H, s, H-27), 0.97 (3H, s, H-23), 0.94 (3H, s, H-25), 0.94 (3H, s, H-30), 0.90 (3H, s, H-29), 0.81 (3H, s, H-26), 0.77 (3H, s, H-24), 0.75 (1H, d, *J*=12.0 Hz, H-5): for ^{13}C NMR (150 MHz, CD_3OD), see Table1: HR-ESI-MS *m/z* 471.3504 $[M-H]^-$.

Punicanolic acid (3ß, 20ß-Dihydroxytaraxastane-28-oic acid, **3**)

White amorphous powder: $[\alpha]^{26}_D$ +5.8 (*c* 1.0, MeOH): TLC (SiO_2, Hex/EtOAc/MeOH 5 : 5 : 0.1, spot visualization) R*f* 0.57: ^{1}H NMR (600 MHz, DMSO-d_6) δ_H 2.95 (1H, m, H-3), 1.01 (3H, s, H-30), 0.92 (3H, d, *J*=5.0 Hz, H-29), 0.92 (3H, s , H-27), 0.87 (3H, s, H-23), 0.86 (3H, s, H-26), 0.78 (3H, s, H-25), 0.65 (3H, s, H-24): for ^{13}C NMR (150 MHz, DMSO-d_6), see Table1: HR-ESI-MS *m/z* 473.3684 $[M-H]^-$.

2-*O*-Acetylmaslinic acid (**4**)

White amorphous powder: $[\alpha]^{26}_D$ +25.0 (*c* 1.0, MeOH): TLC (SiO_2, Hex/EtOAc/MeOH 5 : 5 : 0.1, spot visualization) R*f* 0.48: ^{1}H NMR (600 MHz, CD_3OD) δ_H 5.24 (1H, dd, *J*=3.5, 3.5 Hz, H-12), 4.94 (1H, m, H-2), 3.15 (1H, d, *J*=9.6 Hz, H-3), 2.85 (1H, dd, *J*=4.2, 13.9, H-18), 2.03 (3H, s, $COCH_3$), 1.16 (3H, s, H-27), 1.05 (3H, s, H-25), 1.04 (3H, s, H-23), 0.94 (3H, s, H-29), 0.90 (3H, s, H-30), 0.85 (3H, s, H-24), 0.81 (3H, s, H-26): for ^{13}C NMR (150 MHz, CD_3OD), see Table1: HR-ESI-MS *m/z* 513.3591 $[M-H]^-$.

Epimaslinic acid (2α, 3α-Dihydroxyolean-12-en-28-oic acid, **5**)

White amorphous solid: $[\alpha]^{26}_{D}$ +108.8 (*c* 1.0, MeOH): TLC (SiO_2, Hex/EtOAc/MeOH 5 : 5 : 0.1, spot visualization) R*f* 0.41: ^{1}H NMR (600 MHz, CD_3OD) δ_H 5.25 (1H, dd, *J*=3.6, 3.6 Hz, H-12), 3.92 (1H, ddd, *J*=3.0, 3.0, 12.0 Hz, H-2), 3.31 (over rapped with the solvent peak, H-3), 2.85 (1H, dd, *J*=6.3, 13.2 Hz, H-18), 2.00 (1H, ddd, *J*=3.9, 13.5, 13.5 Hz, H-16), 1.18 (3H, s, H-27), 0.99 (3H, s, H-23), 0.98 (3H, s, H-25), 0.94 (3H, s, H-29), 0.91 (3H, s, H-30), 0.86 (3H, s, H-25), 0.81 (3H, s, H-25): for ^{13}C NMR (150 MHz, CD_3OD), see Table1: HR-ESI-MS *m/z* 471.3574 $[M-H]^-$.

11-Oxo-maslinic acid (2α,3β-Dihydroxy-11-oxo-18β-olean-12-en-28-oic acid, **6**)

Yellowish amorphous powder: $[\alpha]^{26}_{D}$ +49.2 (*c* 1.0, MeOH): TLC (SiO_2, Hex/EtOAc/MeOH 5 : 5 : 0.1, spot visualization) R*f* 0.15: ^{1}H-NMR (600 MHz, CD_3OD) δ_H 5.55 (1H, s, H-12), 3.66 (1H, ddd, *J*=4.2, 9.6, 9.6 Hz, H-2β), 3.08 (1H, dd, *J*=4.2, 12.6 Hz, H-1), 3.00 (1H, dd, *J*=3.6, 13.8 Hz, H-18), 2.92 (1H, d, *J*=9.6 Hz, H-3α), 2.48 (1H, s, H-9), 2.14 (1H, ddd, *J*=4.2, 13.4, 13.4 Hz, H-25), 1.46 (3H, s, H-27), 1.17 (3H, s, H-25), 1.02 (3H, s, H-23), 0.98 (3H, s, H-26), 0.96 (3H, s, H-30), 0.95 (3H, s, H-29) 0.84 (1H, dd, *J*=1.6, 11.7 Hz, H-5), 0.82 (3H, s, H-24): ^{13}C-NMR (150 MHz, CD_3OD), see Table1: HR-ESI-MS *m/z* 487.2911 $[M+H]^+$, *m/z* 485.3356 $[M-H]^-$

Luteolin (**7**)

Yellow amorphous powder: $[\alpha]^{26}_{D}$ +0 (*c* 1.0, MeOH): ^{1}H NMR (600 MHz,

CD_3OD) δ_H 7.38 (1H, dd, *J*=2.4, 8.4 Hz, H-6'), 7.37 (1H, d, *J*=2.4 Hz, H-2'), 6.90 (1H, d, *J*=8.4 Hz, H-5'), 6.54 (1H, s, H-3), 6.44 (1H, d, *J*=2.4 Hz, H-8), 6.21 (1H, d, *J*=2.4 Hz, H-6): ^{13}C NMR (150 MHz, CD_3OD) δ_C 183.9 (C, C-4), 166.4 (C, C-7), 166.1 (C, C-5), 163.3 (C, C-2), 159.5 (C, C-9), 151.0 (C, C-4'), 147.1 (C, C-3'), 123.8 (C, C-1'), 120.3 (CH, C-6'), 116.8 (CH, C-5'), 114.2 (CH, C-2'), 105.4 (C, C-10), 103.9 (CH, C-3), 100.2 (CH, C-6), 95.0 (CH, C-8): HR-ESI-MS *m/z* 287.0392 $[M+H]^+$, *m/z* 285.0428 $[M-H]^-$.

p-Hydroxy-benzoic acid (**8**)

Transparent amorphous solid: $[\alpha]^{26}_D$ +6.8 (*c* 1.0, MeOH): ^1H NMR (600 MHz, CD_3OD) δ_H 7.87 (2H, d, *J*=9.0 Hz, H-2, 6), 6.80 (2H, d, *J*=9.0 Hz, H-3, 5): ^{13}C NMR (150 MHz, CD_3OD) δ_C 170.7 (C-7), 163.2 (C-4), 133.0 (C-2, 6), 123.4 (H-1), 116.0 (H-3, 5): HR-ESI-MS *m/z* 137.0265 $[M-H]^-$.

4-Hydroxy-3-methoxy-benzoic acid, vanillic acid (**9**)

Brownish amorphous solid: $[\alpha]^{26}_D$ +5.0 (*c* 1.0, MeOH): ^1H NMR (600 MHz, CD_3OD) δ_H 7.55 (1H, d, *J*=1.8 Hz, H-2), 7.54 (1H, dd, *J*=1.8, 7.8 Hz, H-6), 6.83 (1H, d, *J*=7.8 Hz, H-5), 3.89 (3H, s, H-8): ^{13}C NMR (150 MHz, CD_3OD) δ_C 170.5 (C-7), 152.6 (C-4), 148.7 (C-3), 125.2 (C-6), 115.9 (C-5), 113.9 (C-2), 56.4 (C-8): HR-ESI-MS *m/z* 169.0649 $[M+H]^+$, *m/z* 167.1366 $[M-H]^-$.

p-Coumaric acid (**10**)

Transparent solid: $[\alpha]^{26}_D$ +5.5 (*c* 1.0, MeOH): ^1H NMR (600 MHz, DMSO-d_6)

δ_H 7.50 (2H, d, *J*=9.0 Hz, H-2, 6), 7.48 (1H, d, *J*=15.6 Hz, H-7), 6.79 (2H, d, *J*=9.0 Hz, H-3, 5), 6.28 (1H, d, *J*=15.6 Hz, H-8): ^{13}C NMR (150 MHz, DMSO-d_6) δ_C 167.9 (C-9), 159.5 (C-4), 143.9 (C-7), 129.9 (C-2, 6), 125.2 (C-1), 115.6 (C-3, 5, 8): HR-ESI-MS *m/z* 165.0686 $[M+H]^+$, *m/z* 163.0426 $[M-H]^-$.

Table 11 ^{13}C NMR data for isolated triterpenes **1-6**

Position	1[a]	2[a]	3[b]	4[a]	5[a]	6[a]
1	48.2	39.9	38.3	45.1	42.5	49.1
2	69.5	27.9	27.0	74.0	67.2	69.2
3	84.5	79.8	76.7	81.0	80.1	84.2
4	40.5	39.9	38.2	40.6	39.5	40.6
5	56.7	56.8	54.7	56.6	49.0	56.2
6	19.6	19.6	17.9	19.6	19.2	18.7
7	33.9	33.9	37.1	33.6	33.9	32.3
8	40.6	40.6	40.6	41.0	40.8	45.1
9	49.0	49.1	48.5	49.0	49.0	63.0
10	39.3	38.2	37.2	39.5	39.5	39.4
11	24.7	24.6	21.1	24.6	24.6	202.7
12	123.5	123.7	28.5	123.4	123.5	128.3
13	145.4	145.3	40.0	145.4	145.3	172.9
14	43.0	42.9	42.1	43.0	43.1	46.5
15	28.8	28.9	28.8	28.8	28.9	28.9
16	24.0	24.1	34.7	24.0	24.1	23.9
17	47.7	47.7	49.3	47.3	47.7	47.2
18	42.8	42.8	46.3	42.8	42.8	43.4
19	47.3	47.3	38.5	47.7	47.4	45.6
20	31.7	31.7	71.1	31.7	31.7	31.7
21	34.9	35.0	36.4	34.9	35.0	34.8
22	34.0	34.1	32.4	33.6	33.9	34.0
23	29.3	28.8	28.0	29.2	29.3	29.3
24	17.1	16.4	15.7	17.7	22.5	17.5
25	17.5	15.9	15.9	16.9	16.9	18.0
26	17.8	17.8	16.1	17.4	17.8	19.9
27	26.5	26.4	14.6	26.4	26.5	24.0
28	181.9	181.9	177.6	181.9	182.1	180.9
29	33.6	33.6	18.1	33.9	33.6	33.0
30	24.1	24.0	29.9	24.1	24.0	23.8
$\underline{C}OCH_3$				173.1		
$CO\underline{C}H_3$				21.4		

[a] ^{13}C NMR measured in CD_3OD

[b] ^{13}C NMR measured in DMSO-d_6

3-3-3. Anti-allergic activity

The anti-allergic activity of the ten isolated compounds was evaluated (Table 12). First, the CC_{50} and CC_{10} were tested at the final concentration of 100 μM or lower. The anti-allergic activity was then tested at the final concentrations lower than the CC_{10}. Ursolic acid as a positive control showed high anti-allergic activity with the IC_{50} value of 39.4 ± 9.9 μM and a CC_{10} value >100 μM.

Among the isolated compounds, the new compound, 11-oxo-maslinic acid (**6**), showed anti-allergic activity with the IC_{50} value 80.6 ± 10.6 μM and the IC_{40} value 71.5 ± 30.0 μM, which was approx. one-half strength of the activity of ursolic acid, and with a CC_{50} value >100 μM. 2-*O*-Acetylmaslinic acid (**4**) affected the anti-allergic reaction of the cells to some degree, with the IC_{40} value 5.9 ± 2.4 μM, the CC_{10} value 17.6 ± 3.4 μM and the CC_{50} value 71.3 ± 7.4 μM. Luteolin (**7**), which is the famous anti-allergic flavone, showed strong activity with the IC_{50} value 10.3 ± 1.6 μM, the IC_{40} value 9.5 ± 1.6 μM and the CC_{50} and CC_{10} value >100 μM. For the other compounds, anti-allergic activity was not detected by epimaslinic acid (**5**) or maslinic acid (**1**) at the concentrations lower than the CC_{10} (IC_{40}, IC_{50} >9.2 μM and IC_{40}, IC_{50} >28.3 μM, respectively). Oleanolic acid (**2**) had no effect on the anti-allergic activity (IC_{40}, IC_{50} >100 μM, CC_{10}, CC_{50} >100 μM). Punicanolic acid (**3**) precipitated in the medium at higher concentration, and we thus evaluated the IC_{50} and CC_{50} values at the soluble concentration, but it showed no activity (IC_{40}, IC_{50} >51.6 μM, CC_{10}, CC_{50} >51.6 μM). *p*-Hydroxy benzoic acid (**8**), vanillic acid (**9**) and *p*-coumaric acid (**10**) showed no effect on the activity (IC_{40},

Table 12 The anti-allergic activity (IC_{50} and IC_{40}) and cytotoxicity (CC_{50} and CC_{10}) of the isolated compounds

Compound	IC_{50} (μM)	IC_{40} (μM)	CC_{50} (μM)	CC_{10} (μM)
Maslinic acid (**1**)	>28.3[Tox]	>28.3[Tox]	>100	28.3 ± 2.8
Oleanolic acid (**2**)	>100	>100	>100	>100
Punicanolic acid (**3**)	>51.6[Pre]	>51.6[Pre]	>51.6[Pre]	>51.6[Pre]
2-*O*-Acetylmaslinic acid (**4**)	>17.6[Tox]	5.9 ± 2.4	71.3 ± 7.4	17.6 ± 3.4
Epimaslinic acid (**5**)	>9.2[Tox]	>9.2[Tox]	>100	9.2 ± 1.0
11-Oxo-maslinic acid (**6**)	80.6 ± 10.6	71.5 ± 30.0	>100	>100
Luteolin (**7**)	10.3 ± 1.6	9.5 ± 1.6	>100	>100
p-Hydroxy benzoic acid (**8**)	>100	>100	>100	>100
Vanillic acid (**9**)	>100	>100	>100	>100
p-Coumaric acid (**10**)	>100	>100	>100	>100
Ursolic acid	39.4 ± 9.9	25.7 ± 1.5	>100	>100

[Tox] The exact value was not determined because of cytotoxicity

[Pre] The exact value was not determined because the compound precipitated in the medium

IC_{50} >100 μM, CC_{10}, CC_{50} >100 μM).

3-4. Discussion

Ten compounds including one new compound were isolated from the EtOH extract of OMW. Among the isolated compounds, 2-*O*-acetylmaslinic acid (**4**), the new triterpene, 11-oxo-maslinic acid (**6**) and luteolin (**7**) were evaluated as an anti-allergic compounds. In the comparison of the structures of the tested triterpenes, it was suspected that there were some important substructures for the anti-allergic activity.

First, among the isolated compounds, 11-oxo-maslinic acid (**6**) and 2-*O*-acetylmaslinic acid (**4**) showed anti-allergic activity. In comparison with the structure of maslinic acid (**1**), the ketone at C-11 of 11-oxo-maslinic acid (**6**) and the acetyl group at C-2 of 2-*O*-acetylmaslinic acid (**4**) would be effective for the anti-allergic activity. As the next step, it should be determined whether the ketone at C-11 and the ketone of acetyl at C-2 play the same role in the anti-allergic activity, that is, in the target protein of these active triterpenes and with the mechanism of action.

This paper is the first report of anti-allergic triterpenes in OMW, and our present findings revealed that not only the phenolic compounds which were reported to date but also some triterpenes in OMW relate to the anti-allergic activity of OMW extract. Until now, the focus has been on polyphenols such as luteolin, apigenin and 3,4-DHPEA-EA as anti-allergic agents of olive oil or OMW, but triterpenes in OMW are also worth investigating, and they have the potential to be useful in functional ways such as food and cosmetic additives or drug development.

To the best of our knowledge, there are only a few reports about the effect of triterpenes on ß-hexosaminidase release and its structure-activity relationship, whereas the structure-activity relationship of flavonoids, stilbenes, and curcuminoids have been summarized (Matsuda et al. 2016). Triterpenes are also widely distributed in natural products, plants and mushrooms, and different types of triterpenes have been found in these materials. More research should be conducted to obtain a comprehensive understanding of the anti-allergic effect of natural triterpenes as well as olive triterpenes, in part because humans consume triterpenes from their daily food. Our present findings of a new anti-allergic triterpene from OMW and the steric structures that are effective for the anti-allergic activity help clarify the useful characteristics of triterpenes and OMW for anti-allergic treatment.

References

Aburjai T, Natsheh FM. 2003. Plants used in cosmetics. *Phytotherapy Res* **17**: 987-100.

Arung TE, Furuta S, Ishikawa H, Kusuma IW, Shimizu K, Kondo R. 2010. Anti-melanogenesis properties of quercetin- and its derivative-rich extract from *Allium cepa*. *Food Chem* **124**: 1024-1028

Arung TE, Shimizu K, Kondo R. 2007. Structure activity relationship of prenylsubstituted polyphenols from *Artocarpus heterophyllusas* inhibitors of melanin biosynthesis in cultured melanoma cells. *Chem Biodiversity* **4**: 2166-2171.

Ashour, A.; Amer, M.; Marzouk, A.; Shimizu, K.; Kondo, R.; EI-Sharkawy, S. Corncobs as apotential source of functional chemicals. *Molecules* **2013**, 18, 13823-13830; doi:10.3390/molecules181113823.

Bollag J, Liu S, Minard, R.D. Enzymatic oligomerization of vanillic acid. *Soil Biology and Biochemistry* **1982**, 14, 157-163.

Brahmi F, Mechri B, Dhibi M, Hammami M. 2013. Variations in phenolic compounds and antiradical scavenging activity of Olea europaea leaves and fruits extracts collected in two different seasons. *Ind Crops Prod* **49**: 256-264.

Budiyanto A, Ahmed NU, Wu A, Bito T, Nikaido O, Osawa T, Ueda M, Ichihashi M. 2000. Protective effect of topically applied olive oil against photocarcinogenesis following UVB exposure of mice. *Carcinogenesis* **21**: 2085-2090.

Covas MI, Nyyssonen K, Poulsen HE. 2006. The effect of polyphenols in olive oil on heart disease risk factors. *Ann Int Med* **145**: 333-431.

Dao JH, Kurzeja RJM, Morachis JM, *et al.* 2009. Kinetic characterization and identification of a novel inhibitor of hypoxia-inducible factor prolyl hydroxylase 2 using a time-resolved fluorescence resonance energy transfer-based assay technology. *Anal Biochemistry* **384**: 213-223.

Decorps J, Saumet JL, Sommer P, Sigaudo-Roussel D, Fromy B. 2014. Effect of ageing on tactile transduction processes. *Aging Res Rev* **13**: 90-99.

Denda M, Tomitaka A, Akamatsu H, Matsunaga K (2003) Altered distribution of calcium in facial epidermis of aged adults. J Invest Dermatology Letter 1557-1558.

Giner E, Recio MC, Rios JL, Giner RM. 2013. Oleuropein protects against dextran sodium sulfate-induced chronic colitis in mice. *J Nat Prod* **76**: 1113-1120.

Ghanbari R, Anwar F, Alkharfy KM, Gilani AH, Saari N. 2012. Valuable nutrients and functional bioactives in different parts of olive (*Olea europaea* L.)–A review. *Int J Mol Sci* **13**: 3291-3340.

Guoying Qiu and Zequan Ji (2014) AngII-induced glomerular mesangial cell proliferation inhibited by losartan via changes in intracellular calcium ion concentration. *Clin Exp Med* 14: 169-176.

Ha JY, Choi HK, Oh MJ, Choi HY, Park CS, Shin HS. 2009. Photo-protective and anti-melanogenic effect from phenolic compound of olive leaf (Olea europaea L. var. Kalamata) extracts on the immortalized human keratinocytes and B16F1 melanoma cells. *Food Sci Biotechnol* **18**: 1193-1198.

Ikawati Z, Wahyuono S, Maeyama K. 2001. Screening of several Indonesian medicinal plants for their inhibitory effect on histamine release from RBL-2H3 cells. *J Ethnopharmacology* **75**: 249-256.

Julia AS (2013) Epidermal barrier formation and recovery in skin disorders. J Clin Invest 116:1150-1158.

Klen TJ, Vodopivec BM. 2012. The fate of olive fruit phenols during commercial olive oil processing: Traditional press versus continuous two- and three-phase centrifuge.

Food Sci Technol **49**: 267-274.

Lin SJ, Defossez PA, Guarente L. 2000. Requirement of NAD and SIR2 for life-span extension by calorie restriction in Saccharomyces cerevisiae. *Science* **289**: 2126-2128.

McCay CM, Crowell MF, Maynard LA. 1935. The effect of retarded growth upon the length of life span and upon the ultimate body size. *J Nutr* **10**: 63-79.

McGrath JA, Robinson MK, Binder RL. 2012. Skin differences based on age and chronicity of ultraviolet exposure: results from a gene expression profiling study. *Br J Dermatol* **166**: 9-15.

Mijatovic SA, Timotijevic GS, Milijkovic DM, *et al*. 2010. Multiple antimelanoma potential of dry olive leaf extract. *Int J Cancer* **128**: 1955-1965.

Miller LS, Cho JS. 2011. Immunity against Staphylococcus aureus cutaneous infections. *Nat Rev Immunol* **11**: 505-518.

Mira A, Tanaka A, Tateyama Y, Kondo R, Shimizu K. 2013. Comparative biological study of roots, stem, leaves, and seeds of *Angelica shikokiana* Makino. *J Ethnopharmacology* **148**: 980-987.

Obied HK, Bedgood DR, Prenzler PD, Robards K. (2007) Chemical screening of olive biophenol extractsby hyphenated liquid chromatography. *Analytica Chemica Acta* 603: 176-189.

Perez-Bonilla M, Salido S, van Beek TA, Linares-palomino PJ, Altarejos J, Nogueras M. (2006) Isolation and identification of radical scavengers in olive tree (*Olea europaea*) wood. *J Chromarogr A* 111: 311-318.

Rafehi H, Smith AJ, Balcerczyk A, et al. 2012. Investigation into the biological properties of the olive polyphenol, hydroxytyrosol: mechanistic insights by genome-wide mRNA-Seq analysis. *Genes Nutr* **7**: 343-355.

Romero C, Garcia P, Brenes M, Garcia A, Garrido A. 2002. Phenolic compounds in natural black Spanish olive varieties. *Eur Food Res Technol* **215**: 489-496.

Sato A, Shinozaki N, Tamura H. 2014. Secoiridoid type of antiallergic substances in olive waste materials of three Japanese vatieties of *Olea europaea*. *J Agric Food Chem* **62**: 7787-7795.

Tanaka A, Zhu Q, Tan H, *et al*. 2014. Biological Activities and Phytochemical Profiles of Extracts from Different Parts of Bamboo (*Phyllostachys pubescens*). *Mol* **19**: 8238-8260.

Thaipong K, Boonprakob U, Crosby K, Cisneros-Zevallos L, Byrne DH. 2006. Comparison of ABTS, DPPH, FRAP, and ORAC assays for estimating antioxidant activity from guava fruit extracts. *J Food Composition Anal* **19**: 669-675.

Tao Sun, Fei Ye, Hong Ding, Kaixian Chen, Hualiang Jiang, Xu Shen (2006) Protein tyrosine phosphatase 1B regulates TGFß1-induced Smad2 activation through PI3 kinase-dependent pathway. *Cytokine* 35: 88-94.

Tsutsumi M, Goto M, Denda M (2013) Dynamics of intracellular calcium ion cultured human keratinocytes after localized cell damage. Experimental Dermatology 22: 358-379.

Yamauchi K, Mitsunaga T, Batubara I. 2013. Novel quercetin glucosides from *Helminthostachys zeylanica* root and acceleratory activity of melanin biosynthesis. *J Nat Med* **67**: 369-374.

Cardoso S M, Falcao S I, Peres A M, Domingues M R M (2011) Oleuropein/ligstroside isomers and their derivatives in Portuguese olive mill wastewaters. Food Chem 129: 291-296. doi: 10.1016/j.foodchem.2011.04.049.

Cromheecke J L, Nguyen K T, Huston D P (2014) Emerging role of human basophil biology in health and disease. Curr Allergy Asthma Rep 14: 408. doi: 10.1007/s11882-013-0408-2.

Fernandez-Hernandez A, Martinez A, Rivas F, Garcia-Mesa J A, Parra A (2015) Effect of the solvent and the sample preparation on the determination of triterpene compounds in two-phase olive-mill-waste samples. J Agric Food Chem 63: 4269-4275.

Flamini, G.; Antognoli, E.; Morelli, I. Two flavonoids and other compounds from the aarial parts of *Centaurea bracteata* from Italy. *Phytochemistry* **2001**, 57, 559-564.

Harvima I T, Levi-Schaffer F, Draber P, Friedman S, Polakovicova I, Gibbs B F, Blank U, Nilsson G, Maurer M (2014) Molecular targets on mast cells and basophils for novel therapies. J Allergy Clin Immunol 134: 530-543. doi: 10.1016/j.jaci.2014.03.007.

Isoda H, Motojima H, Margout D, Neves M, Han J, Nakajima M, Larroque M (2012) Antiallergic effect of *Picholine* olive oil-in-water emulsions through ß-hexosaminidase release inhibition and characterization of their physicochemical properties. J Agric Food Chem 60: 7851-7858. doi: 10.1021/jf3016078.

Kishikawa A, Ashour A, Zhu Q, Yasuda M, Ishikawa H, Shimizu K (2015) Multiple biological effects of olive oil by-products such as leaves, stems, flowers, olive milled

waste, fruit pulp, and seeds of olive plant on skin. Phytotherapy Res 29: 877-886. doi:10.1002/ptr.5326.

Klen T J, Vodopivec B M (2012) The fate of olive fruit phenols during commercial olive oil processing: Traditional press *versus* continuous two- and three-phase centrifuge. LWT – Food Sci Technol 49: 267-274. doi: 10.1016/j.lwt.2012.03.029.

Mahato SB, Kundu AP (1994) ^{13}C NMR spectra of pentacyclic triterpenoids—a compilation and some salient features. Phytochem 37: 1517-1575.

Martinez A, Rivas F, Perojil A, Parra A, Garcia-Granados A, Fernandez-Vivas A (2013) Biotransformation of oleanolic and maslinic acids by *Rhizomucor miehei*. Phytochem 94: 229-237.

Matsuda H, Nakamura S, Yoshikawa M (2016) Degranulation inhibitors from medicinal plants in antigen-stimulated rat basophilic leukemia (RBL-2H3) cells. Chem Pharm Bull 64: 96-103.

Miyazawa, M.; Hisama, M. Antimutagenic activity if flavonoids from *Chrysanthemum morifolium*. *Bioscience, Biotechnology, and Biochemistry* **2003**, 67, 2091-2099.

Murata K, Abe Y, Shinohara K, Futamura-Masuda M, Uwaya A, Isami F, Matsuda H

(2014) Anti-allergic activity of the *Morinda citrifolia* extract and its constituents. Pharmacogn Res 6: 260-265. doi: 10.4103/0974-8490.132608.

Rubio-Senent F, Rodriguez-Gutierrez G, Lama-Munoz A, Garcia A, Fernandez-Bolanos J (2015) Novel pectin present in new olive mill wastewater with similar emulsifying and better biological properties than citrus pectin. Food Hydrocolloid 50: 237-246.

Rudiyansyah, Garson MJ (2006) Secondary metabolites from the wood bark of *Durio zibethinus* and *Durio kutejensis*. J Nat Prod 69:1218-1221. doi: 10.1021/np050553t.

Sanchez-Quesada C, Lopez-Biedma A, Warleta F, Campos M, Beltran G, Gaforio J J (2013) Bioactive properties of the main triterpenes found in olives, virgin olive oil, and leaves of *Olea europaea*. J Agric Food Chem 61: 12173-12182.

Sato A, Shinozki N, Tamura H (2014) Secoiridoid type of antiallergic substances in olive waste materials of three Japanese varieties of *Olea europaea*. J Agric Food Chem 62: 7787-7795. doi: 10.1021/jf502151b.

Sengab A.E.B., El nagger D.M.Y., Elgindi M.R., Elsaid M.B. (2015) Biological studies of isolated triterpenoids and phenolic compounds identified from *Wodyetia bifurcata* family Arecaceae. *Journal of Pharmacognosy and Phytochemistry* 3: 67-73.

Siracusa M C, Kim B S, Spergel J M, Artis D (2013) Basophils and allergic inflammation. J Allergy Clin Immunol 132: 789-801. doi: 10.1016/j.jaci.2013.07.046.

Tanaka JCA, Vidotti GJ, Silva CC (2003) A new tormentic acid derivative from *Luehea divaricata* Mart. (Tiliaceae). J Braz Chem Soc 14: 475-478. doi: 10.1590/S0103-50532003000300024.

Thoison O, Sevent T, Niemeyer HM, Russell GB (2004) Insect antifeedant compounds from *Nothofagus dombeyi* and *N. pumilio*. Phytochem 65: 2173-2173.

Watt FM (1989) Terminal differentiation of epidermal keratinocytes. Current Opinion in Cell Biology 1: 1107-1115.

Wen X, Sun H, Liu J, Cheng K, Zhang P, Zhang L, Hao J, Zhang L, Ni P, Zographos SE, Lenoidas DD, Alexacou K, Gimisis T, Hayes JM, Oikonomakos NG (2008) Naturally occurring pentacyclic triterpenes as inhibitors of glycogen phosphorylase: synthesis, structure-activity relationships, and X-ray crystallographic studies. J Med Chem 51: 3540-3554.

Wu Z, Uchi H, Morino-Koga S, Shi W, Furue M (2014) Resveratrol inhibition of human keratinocyte proliferation via SIRT1/ARNT/ERK dependent downregulation of aquaporin 3. J Dermatol Sci. doi: 10.1016/j.jdermsci.2014.03.114.

Xie Y, Morikawa T, Ninomiya K, Imura K, Muraoka O, Yuan D, Yoshikawa M (2008) Medicinal flowers. XXIII. New taraxastane-type triterpene, punicanolic acid, with tumor necrosis factor-✔ inhibitory activity from the flowers of *Punica granatum*. Chem Pharm Bull 56: 1628-1631.

Youn UJ, Lee YJ, Jeon HR, Shin HJ, Son YM, Nam J, Han A, Seo E (2010) A pyridyl alkaloid and benzoic acid derivatives from the rhizomes of *Anemarrhena asphodeloides*. Natural Product Sciences 16: 203-206.